

# Opportunistic scheduling of wind farm O&M activities using forecasting of power markets and curtailment periods

Master Thesis

Johan Østergaard Knarreborg & Jonathan Hjortshøj-Nielsen



## Abstract

The transition to renewable energy is essential for mitigating climate change, and offshore wind farms (OWFs) are key contributors to this effort. The operations and maintenance (O&M) activities of OWFs account for up to 30% of their total lifetime costs. This study aims to optimize O&M activities by integrating day-ahead power market price forecasts into an opportunistic O&M scheduling framework to strategically schedule maintenance during periods of low revenue.

Multiple power market forecasting methodologies including statistical and ML approaches are integrated into a Mixed Integer Linear Program (MILP) operations research (OR) model to create a realistic and detailed 15-minute schedule that obeys the physical layout of the wind farm, Crew Transfer Vessel (CTV) routing optimized for fuel efficiency and crew placement. Kriegers Flak OWF, located in the Baltic Sea and owned by Vattenfall, serves as the case study for the proposed model.

The results indicate that aligning maintenance with periods of forecasted low revenue can substantially reduce lost revenue due to maintenance related shutdowns. Applying the model to Kriegers Flak demonstrates a potential reduction in lost revenue due to scheduled maintenance (SM) by up to 79.4% compared to a naive scheduling method. Sensitivity analyses confirm the model's robustness across varying input parameters, suggesting its applicability to diverse wind farm configurations.

This study presents a novel approach to OWF O&M optimization by integrating power market price forecasts with opportunistic maintenance scheduling. The findings highlight the economic benefits of maximizing revenue availability rather than uptime or production availability. Future work should refine the model for increased realism and validate results across other OWFs and OWF sizes to establish broader applicability. In conclusion, this study contributes to making OWFs more financially viable and supports the green energy transition through improved O&M efficiency and reduced costs.

## Acknowledgements

**Stefan Røpke**, Professor, Department of Technology, Management and Economics DTU. Internal DTU advisor, providing invaluable guidance within Operations Research and project

**Thor Heine Snedker**, Senior Consultant, Peak Wind

External Advisor, Providing Offshore Wind insights and valuable feedback on model development.

**Ilmas Bayati**, Head of Operations Economics & Analytics, Peak Wind

External Advisor, Providing Offshore Wind insights and valuable feedback on model development.

**Jade McMorland**, Consultant, Peak Wind

Technical advisor, Provided technical expertise on O&M activities based on her academic work related to the project.

# Contents

Acknowledgements . . . . .	II
<b>1 Introduction</b>	<b>1</b>
<b>2 Abbreviations</b>	<b>3</b>
<b>3 Literature Review</b>	<b>4</b>
3.1 Offshore O&M . . . . .	4
3.2 OR scheduling methods . . . . .	5
3.3 Forecasting methods . . . . .	6
<b>4 Methodology</b>	<b>8</b>
4.1 Case study: Kriegers Flak . . . . .	8
4.2 Data . . . . .	9
4.3 Forecasting . . . . .	11
4.4 O&M Model . . . . .	18
4.5 Computation - High Performance Compute . . . . .	32
4.6 Analysis of model . . . . .	33
4.7 Methods Compared . . . . .	34
4.8 CO <sub>2</sub> savings . . . . .	37
<b>5 Results</b>	<b>38</b>
5.1 Forecasts . . . . .	38
5.2 Tuning hyper parameters . . . . .	40
5.3 Computations . . . . .	43
5.4 Short- and long-term simulations . . . . .	46
5.5 Profit increase per MW installed capacity . . . . .	57
5.6 Sensitivity Analysis . . . . .	58
<b>6 Discussion</b>	<b>61</b>
6.1 OR model architecture . . . . .	61
6.2 Hyper parameter tuning . . . . .	61
6.3 O&M Model Performance . . . . .	64
6.4 Sensitivity analysis . . . . .	67
6.5 Effectiveness of optimization given PPAs or CFDs . . . . .	68
6.6 Broader impact . . . . .	68
6.7 Key benefits of the proposed O&M model . . . . .	69

6.8	Model limitations . . . . .	70
6.9	Future work . . . . .	72
6.10	Conclusion . . . . .	75
	<b>Bibliography</b>	<b>76</b>
	<b>A Appendix</b>	<b>80</b>
A.1	Detailed tables . . . . .	80
A.2	Unit check . . . . .	83
A.3	GitHub Link . . . . .	83

# 1 Introduction

The transition to renewable energy sources is an essential step in the move towards substituting fossil fuels for renewable energy sources and mitigating climate change. Offshore Wind Farms (OWF) have emerged as a key technology already offering a substantial source of clean energy. OWFs operate in hostile environments and the operations and maintenance (O&M) activities presents a significant logistic and financial burden. O&M activities accounting for up to 30% of total lifetime cost (Röckmann, Lagerveld, and Stavenuiter 2017). The substantial share of costs stemming from O&M activities underscores the importance of optimizing this key element in order to rely on offshore wind in the green transition.

The significance of optimizing O&M related activities is further highlighted by the increase in volatility and rising electricity prices since the energy crisis in late 2021 (Erkan, Ergüney, and Gürsoy 2022). This volatility requires power producers to maximize power sales during periods of high production and high prices and strategically schedule maintenance in periods of not just low production but more importantly low revenue. Efficiently optimizing O&M activities for OWFs not only reduces costs related to O&M activities but supports the broader goal of the green transition by making OWFs more cost-efficient and thereby renewable energy source a more attractive investment.

This study addresses the need for reducing O&M related cost by implementing day-ahead power market price forecasts into an opportunistic O&M scheduling framework. The objective is to develop a scheduling model that enables OWF operators to strategically place maintenance activities in periods of low revenue and thereby maximize revenue rather than maximize uptime or production. Kriegers Flak OWF, owned by Vattenfall and located in the Baltic sea, serves as a case study for testing the developed model.

The proposed model employs and tests multiple power market forecasting methodologies, including a combination of Long Short-Term Memory (LSTM) neural networks and Extreme Gradient Boosting (XGBoost) models, Exponentially Weighted Moving Average (EWMA), and Auto-Regressive Integrated Moving Average with Exogenous variables (ARIMAX) models. The forecasts are integrated into a Mixed Integer Linear Program (MILP) operations research (OR) model. Here the physical layout of the wind farm, together with CTV routing and crew placement is modelled in a realistic schedule obeying the physical constraints of the specific OWF. The model leverages historical weather and price data to back-test the developed strategies for 2021 and 2022.

The results show that by aligning maintenance with periods of forecasted low revenue

OWFs can substantially reduce the lost revenue due to maintenance related shutdowns. The application of the model to Kriegers Flak demonstrates a potential reduction in lost revenue due to scheduled maintenance by up to 79.4% compared to a Naive method of placing maintenance without a revenue forecast. A benefit, although smaller, is also seen when comparing the proposed model to a production-maximizing strategy. Sensitivity analyses confirm the robustness of the model across varying input parameters suggesting its applicability to diverse wind farm configurations.

This study contributes to the body of research on offshore wind farm operations by presenting a novel and comprehensive model that integrates power market price forecast with an opportunistic O&M strategy. The results underline the economic benefit of maximizing revenue availability rather than uptime or production. Additional work should go into refining the model to increase its realism. Moreover, further validation of results on other OWFs would help establish the added benefit when extrapolating results to other wind farms.

In conclusion, this study highlights the significant potential cost savings and efficiency improvements in O&M for OWFs through the application of power market price forecasting in combination with an opportunistic maintenance model to optimize revenue availability. By addressing this major cost factor for one of the key renewable energy sources, this study hopes to contribute to more financially viable OWFs and thereby the green energy transition.

## 2 Abbreviations

Table 2.1: Report abbreviations

Abbreviation	Definition
MILP	Mixed Integer Linear Program
O&M	Operations and Maintenance
OR	Operations Research
CBM	Condition-based Maintenance
CMS	Corrective Maintenance Strategy
CM	Corrective Maintenance
PrM	Predictive Maintenance
PM	Preventive Maintenance
OM	Opportunistic Maintenance
SM	Scheduled Maintenance
KPI	Key Performance Indicator
LCOE	Levelized Cost of Energy
CTV	Crew Transfer Vessel
NWP	Numerical Weather Prediction
ANN	Artificial Neural Network
LSTM	Long Short-Term Memory
XGBoost	Extreme Gradient Boosting
TSP	Traveling Salesman Problem
CFD	Contracts for Difference
PPA	Power Purchase Agreement
DK2	Danish Electricity Zone 2
WT	Wind Turbine
ERA5	ECMWF Reanalysis 5th Generation
API	Application Programming Interface
RMSE	Root Mean Square Error

# 3 Literature Review

The increasing focus and reliance on renewable energy sources has driven the expansion of offshore wind energy. Efficient maintenance strategies are essential to operate a wind farm in a reliable and cost-effective way. This literature review outlines the current research within offshore wind operations and maintenance (O&M) activities and highlights relevant operations research (OR) literature on the subject of relevant scheduling and routing methods.

## 3.1 Offshore O&M

Optimization of O&M in offshore wind is a common problem explored in many articles. Xia and Zou (2023) creates an overview of some of the existing maintenance strategies. These include Routine inspection, Condition-based maintenance (CBM), Corrective maintenance (CM), Predictive maintenance (PrM), Preventive maintenance (PM), and Opportunistic maintenance (OM). Often literature combines strategies to further optimize the maintenance strategy (Walger, Peters, and Madlener 2017). For each maintenance strategy, the literature mainly minimizes either costs as in (Walger, Peters, and Madlener 2017; J. Wang, Zhao, and Guo 2019; F. Fallahi et al. 2022; Kang and Guedes Soares 2020; Papadopoulos, Farnaz Fallahi, et al. 2023), maximizes time-based availability as discussed in Lu et al. (2018)) or maximizes production availability as in Erguido et al. (2017). How this study differs from current literature in regards to method used for O&M and OR, evaluation method, and forecasting data is illustrated in table 3.3.

Other articles such as Besnard, Fischer, and Bertling Tjernberg (2013) focus on optimizing the support organisation size for O&M. While this study does not optimize directly for the support organisation size, the size of the support organisation will be investigated.

Opportunistic maintenance is a newer field that has been explored more in recent years as outlined in McMorland et al. (2023). Opportunistic maintenance takes a trigger, either internal or external, as an opportunity to perform scheduled maintenance (SM) or preventive maintenance (PM). The concept of internal and external opportunities can be seen in McMorland et al. (2023). One of the most common internal triggers used is corrective maintenance (CM) giving rise to the opportunity to conduct other maintenance activities (Kang and Guedes Soares 2020; Li et al. 2020). External triggers are most commonly weather opportunities, which is used in a number of opportunistic O&M optimization studies (Erguido et al. 2017; Papadopoulos, Coit, and Ezzat 2022). Using market-based external triggers is not seen often but proposed in McMorland et al. (2023) as OM+, where the market-based availability is optimized rather than time- or

production-availability, also referred to as energy-based availability.

In Papadopoulos, Coit, and Ezzat (2022) a stochastic optimization framework is implemented, where energy prices are taken into account as an opportunity cost. They name these opportunities revenue-based opportunities. The price forecasts used in Papadopoulos, Coit, and Ezzat (2022) are created by a Lasso Estimated Auto-Regressive model that has been proposed in Lago et al. (2021). They work with a planning horizon of 20 days, and contrary to this study's approach, Papadopoulos, Coit, and Ezzat (2022) uses a stochastic approach with results based on 50 scenarios. They obtain an improvement of 52.81% and 68.79% over Condition-Based Scheduling (CBS) and Corrective Maintenance Strategy (CMS) strategies respectively in the overall cost of maintenance.

To simulate the O&M activities of an OWF it is important to have accurate failure rates. Carroll, McDonald, and McMillan (2016) has failure rates for each component type with repair time and repair cost for each type of failure. The failure rates from Carroll, McDonald, and McMillan (2016) are used in multiple papers related to offshore wind maintenance (Kang and Guedes Soares 2020; Papadopoulos, Farnaz Fallahi, et al. 2023; Li et al. 2020; Erguido et al. 2017; Papadopoulos, Coit, and Ezzat 2022; Lu et al. 2018).

## 3.2 OR scheduling methods

In this study an OWF will be modelled, this includes the location of turbines, maintenance crews, and crew transfer vessel (CTV) routing. The problem will be modelled as a mixed integer linear program (MILP) that optimizes the overall operating profit of the OWF. This problem can be considered a case of the Vehicle Routing Problem with Time Windows (VRPTW) as introduced in Kallehauge et al. (2005). Zhang et al. (2017) solves a similar problem using time-space nodes and arcs between each time-space node for a bike-sharing repositioning problem. Here a service vehicle moves between service stations throughout the day (time-space nodes) and are only allowed to travel between time-space nodes with an arc. They assume that each service vehicle has the same capacity, allowing for easy interchange, and fixed distances between nodes throughout the day. The concept of time-space nodes and arcs will directly be applied to this project. Irawan et al. (2017) minimizes the cost of technicians and travel time between turbines using a similar approach.

With a significant amount of nodes in the VRPTW, it can become difficult to solve to optimality. In the literature, the VRPTW has been solved by many heuristic methods as seen in Pisinger and Røpke (2007). In this study, a matheuristic will be developed in order to solve the context specific VRPTW.

### **3.3 Forecasting methods**

Forecasting methods are crucial for planning of O&M activities in offshore wind. In particular forecasts for power market prices as well as weather forecasts are necessary to make accurate and informed decisions based on expected revenue, as this study proposes.

#### **Power market price forecasting**

In power market price forecasting the forecasting horizon is often referred to as being short-, mid- and long-term. Typically, as in K. Wang et al. (2023), short-term forecasts are hourly forecasts that predict the next hourly market price based on previous available information. Mid-term forecasts are typically considered when using a forecasting horizon of a day up to one week as seen in Ziel and Steinert (2018). Finally long-term forecasts are usually with a forecasting horizon of more than one week and can potentially be far into the future (Esteves et al. 2015). This typically also includes fundamental analysis of underlying macroeconomic factors such as demographic development as well as forecasts for electricity consumption etc. as seen in Pessanha and Leon (2015). This study will focus on the medium-term power markets forecasts with a forecasting horizon of up to 4 days. There are two primary power market price forecasting methods. The most used forecasting methods are statistical methods such as autoregressive integrated moving average exogenous (ARIMAX) as in Conejo et al. (2005), however current alternative methods using artificial neural networks (ANN) are able to capture more of the stochastic and volatile nature of the electricity markets as argued in K. Wang et al. (2023). In this study several forecasting methods will be tested, using both statistical and ANN approaches.

#### **Weather & wind power Forecasting**

To successfully run an OWF the operator needs knowledge about future power generation. This allows for correct bids in the power market and knowledge about future revenue. Wind power forecasting can be performed both short-term and long-term. This is typically achieved by a combination of the expected weather conditions and the configuration and condition of the OWF, resulting in a forecast of the expected power production. Short-term wind power forecasting usually relies on wind speed forecasts, as the power produced is very correlated with the wind speed. Tsai et al. (2023) outlines the most common method of wind power forecasting, with the most simple being a physics-based method. In a physics-based method the forecasted wind speed is directly converted to power using the turbine power curve. A physics-based method will be implemented in this study. More advanced methods include statistical or deep learning methods to take historical power output into account when predicting power output from wind speed forecasts. Some of the more advanced methods also account for the turbine wake effect seen in

OWFs (Tsai et al. 2023).

At the core of each of the methods described above, lies a weather forecast, and more specifically a wind speed forecast. The Integrated Forecast System High Resolution (IFS HRES) from European Centre for Medium-Range Weather Forecasts (ECMWF) is one of the most widely used numerical weather predictions (NWP) (European Centre for Medium-Range Weather Forecasts 2024). AI/ML methods have seen a huge improvement in recent years with Google, Nvidia, and Huawei respectively releasing GraphCast, FourCastNet, and Pangu-Weather which are all deep learning models (Lam et al. 2023; Pathak et al. 2022; Bi et al. 2022). While the newly developed AI methods have greatly reduced the necessary computational power and data to create weather forecasts it is still outside the scope of this study. This study will therefore not use NWP or AI methods, but will rely on synthetic wind speed forecasts created by adding random walk noise to the actual weather as explained in section 4.3.

Table 3.1: Overview of relevant O&M literature.

Publication	O&M methodology	OR Methodology		Forecasting methods		Evaluation method
	Maximization of forecasted revenue	Model of physical wind farm	Time-space nodes	Price forecast	Weather forecast	Long run simulations
Papadopoulos, Coit, and Ezzat 2022	✓			✓	✓	✓
Lu et al. 2018						✓
Papadopoulos, Farnaz Fallahi, et al. 2023				✓	✓	✓
Kang and Guedes Soares 2020						
Walgren, Peters, and Madlener 2017						
J. Wang, Zhao, and Guo 2019						
F. Fallahi et al. 2022		✓				
Erguido et al. 2017					✓	
Irawan et al. 2017		✓		✓		
<b>This study</b>	✓	✓	✓	✓	✓	✓

# 4 Methodology

In the following sections the methodologies used in this study will be presented, along with the relevant data to carry out a quantitative analysis of the proposed O&M model.

## 4.1 Case study: Kriegers Flak

In this study Kriegers Flak will be used as a case study to investigate the impact of the proposed opportunistic O&M methodology.

### Physical layout

The Krigers Flak OWF is located in the baltic sea, where it has been providing electricity to the Danish energy market since the summer of 2021. Kriegers Flak is serviced from Klintholm harbour shown in figure 4.1B. The harbour is located between 19-40 km from all turbines. A detailed overview of the OWF specification can be seen in table 4.1.

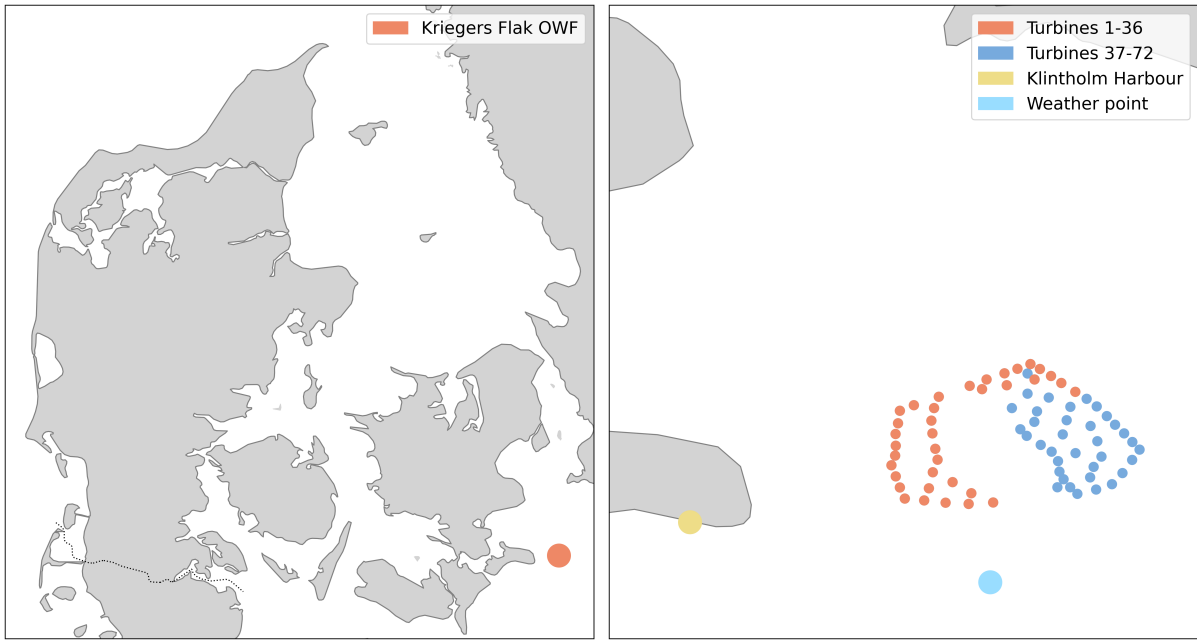
Table 4.1: Kriegers Flak OWF specifications.

Specification	
Location	Baltic sea
Owner & Service provider	Vattenfall
Capacity	604.8 [MWe]
Nr. of turbines	72
WT Type	Siemens Gamesa SWT 8.4-167
O&M Harbour	Klintholm Harbour
Distance from O&M harbour	19-40 Km
Operation start	Summer 2021

The layout and position of Kriegers Flak, seen in figure 4.1, has been provided by Vattenfall. Note that half of the wind turbines are marked in separate colours. This is done to illustrate, which turbines are being considered, when only half of them are used in some of the computationally intensive sensitivity analyses. The weather station in 4.1B is the point location used to retrieve data from the ERA5 dataset.

### Power Curve

As discussed in the literature review, this study will use the power curve of the relevant offshore wind turbine (OWT) to approximate the power production. The power curve for the Siemens Gamesa SWT 8.4-167 is unavailable, however the power curve for the Siemens Gamesa SWT-8.0-167 is available in Diaconita, Andrei, and Rusu (2022). The turbines



(A) Position of Krigers Flak OWF.

(B) Detailed layout of Krigers Flak OWF.

Figure 4.1: Layout of Krigers Flak OWF. Turbines 1-36 will be commonly throughout this study.

are similar in dimensions, but the turbine used at Krigers Flak have a slightly higher rated power of 8.4 MW compared to the 8 MW from the Siemens Gamesa SWT-8.0-167 turbine. The power curve of the Siemens Gamesa SWT-8.0-167 turbine is used, but with the adoption of a maximum rated power of 8.4 MW as seen in figure 4.2.

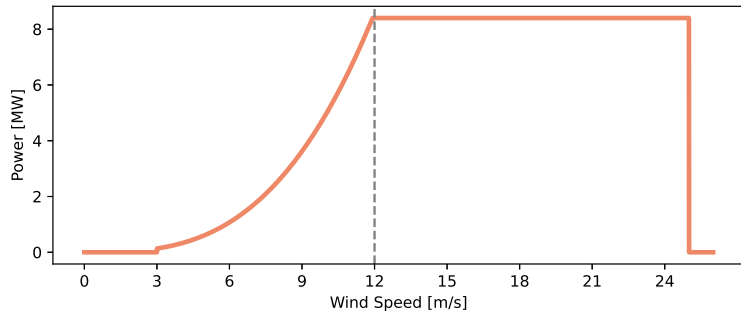


Figure 4.2: Power Curve of the Siemens Gamesa SWT 8.4-167 OWT

This allows for a conversion from wind speed to power production.

## 4.2 Data

Consistent data is crucial for both reliable and realistic results. This section will introduce the key data sources that are required for creating the O&M activity optimization model proposed in this study.

## Weather Data

The weather data has been collected from the Copernicus 'ERA5 hourly data on single levels from 1940 to present' dataset (Hersbach et al. 2023). The ERA5 dataset is a globally spanning weather dataset that includes observations for more than a hundred variables. Only three of these variables are used in this study. The variables used and the corresponding resolution can be seen in table 4.2.

Table 4.2: Weather Data Variables used from the ERA5 dataset.

Variable	Resolution
100m_u_component_of_wind	0.25°x 0.25°
100m_v_component_of_wind	0.25°x 0.25°
significant_height_of_combined_wind_waves_and_swell	0.5°x 0.5°

From the variables shown in table 4.2 the 100 meter altitude absolute wind speed is calculated by equation 4.1.

$$WS_t = \sqrt{(u_t^{100m})^2 + (v_t^{100m})^2} \quad (4.1)$$

Where  $WS_t$  is the absolute wind speed,  $u_t^{100m}$  is the 100 meter  $u$  component of the wind and  $v_t^{100m}$  is the 100 meter  $v$  component of the wind at hour  $t$ . Since the hub height of the Siemens Gemesa SWT 8.4-167 used at Kriegers Flak is 104.5 meters, the 100 meter altitude wind speed is used to calculate power generated by the turbines. The data is retrieved for the coordinates 54.9° N, 12.9° E, which is the data point closest to Kriegers Flak OWF shown in figure 4.1B. Historical wind speed is shown in figure 4.3 A clearly showing higher wind speeds during winter months in the area of Kriegers Flak OWF. The weather data used in the study span the period from 2019 through 2022 as weather data for all of 2023 is unavailable at the time of data collection.

## Electricity price data

Optimizing operations for revenue requires knowledge about electricity prices. Krigers Flak OWF is connected to the Danish and German electricity grid. Due to simplicity only the Danish electricity connection to the DK2 Zone is considered in this project.

Hourly day-ahead electricity prices are fetched from ENTSOE using ENTSOEs RESTful API (ENTSO-E 2024). The day-ahead price is the price the electricity producer receives for the electricity they bid in the day-ahead market. In this project it is assumed that all produced electricity is correctly forecasted, when offers are placed for the total amount produced in the day-ahead market. In this case the hourly day-ahead price is what the

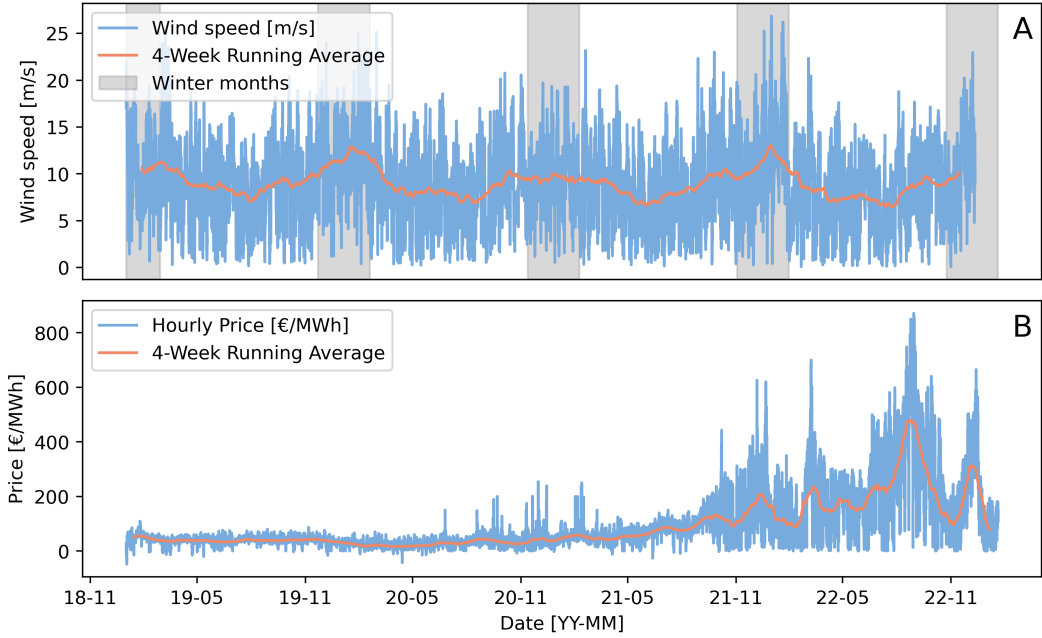


Figure 4.3: A) Historical 100m wind speeds at Kriegers Flak for 2019-2022. Grey time periods represents winter months where wind speeds in general are higher. B) DK2 electricity prices for 2019-2022 clearly illustrating the price increase starting in late 2021.

electricity producer receives for the power produced. Data has been collected for 2019 - 2022. With 2019-2021 being used as training data, and 2022 used as test data. In figure 4.3 B the price development over the four year period can be seen. Here it is important to note the shift in electricity prices especially during latter half of 2021 and 2022 primarily caused by the energy crisis (Erkan, Ergüney, and Gürsoy 2022). This is expected to have an effect on the ability to accurately forecast the power market prices, as the power market forecasting model will not have seen such a shift in market prices in the training data.

### 4.3 Forecasting

To optimize expected revenue of the wind farm, forecasts for both wind and power market prices are needed. Here it is important to discuss the timing of the two forecasts based on the mechanism for placing offers in the day-ahead market in order to sell the expected production including shutdowns due to maintenance. Particularly in the day-ahead market the bids and offers are collected at 12 o'clock noon in and cleared in the following hours on the day before the actual delivery of the power,  $d - 1$ . This must be taken into account when employing the forecasting methods, such that weather observed after 12 o'clock noon is not revealed to the forecaster ahead of time. This will be done by creating a weather forecast at 12 o'clock noon on day  $d - 1$  just before the deadline for placing offers in the day-ahead market. It is assumed in this study that the OWF operator will

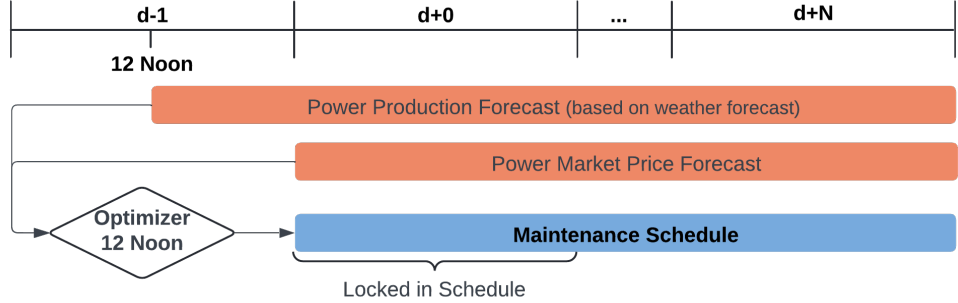


Figure 4.4: Optimization model based on forecasts for day-ahead market prices and expected power production. The Optimization model is run at 12 Noon. Only maintenance schedule for the next day,  $d+0$ , is locked in. For each daily iteration a plan can be made  $N$  days ahead. If only planning one day ahead, then  $N=0$ .

offer their produced power at a price of 0 €/MWh. If the market clearing price is larger than the offer price, the offer is accepted and the OWF operator receives the market clearing price. Thus if negative prices are observed the offer is rejected and no power is sold or delivered.

The forecasted power production-based on the weather forecast and the power market price forecast is provided to the optimization model as seen in figure 4.4. The OR optimization model maximizes the revenue for over the subsequent  $N$  days, where  $N$  is the planning horizon. Only the schedule for the coming day is locked in. The specific forecasting methods for weather and market prices are described in the following sections.

## Curtailment periods

Curtailment is the process by which the grid operator reduces the power production of a producer to stabilize the electricity grid, typically due to grid congestion or a surplus of generation (Schermeyer, Vergara, and Fichtner 2018). This study does not include periods of curtailment in the scheduling of O&M activities. The primary reason for excluding curtailment is the unavailability of specific data, which is sensitive and unique to each power producer. Additionally in the forecasted revenue lies an implicit forecast of the possibility of curtailment. This is due to curtailment periods being associated with lower power market price periods (Schermeyer, Vergara, and Fichtner 2018). Given that the O&M model optimizes revenue it should most likely choose to do maintenance during low price periods and thereby also during potential curtailment periods. Finally curtailment is a relatively rare phenomenon (Nycander et al. 2020).

## Wind Power Forecast

As discussed in the literature review multiple methods exist for generating weather forecasts and wind power forecasts. As many accurate forecasting methods require meteorological domain knowledge, heavy computational resources or a combination of the two,

it is not feasible within the scope of this study to create a forecasting model or utilize the current NWP models in a back-testing manner. Instead the weather forecasts will be based on a method where forecasts are generated based on the true future weather. Here random noise will be added to historical weather to emulate a realistic forecast accuracy based on some of the current industry standard weather forecasting models. The noise is applied by a random walk with an attraction factor to the actual weather following equation 4.2.

$$y_{t+1} = \alpha \cdot \left( 0.8 + 2 \cdot \exp \left( \frac{-(t+1)}{50} \right) + (t+1) \cdot \frac{1}{500} \right) \cdot (x_{t+1} - y_t) + \beta \cdot X + y_t, \quad X \sim N(0, 1) \quad (4.2)$$

Here  $\alpha$  is the attraction factor,  $\beta$  is the strength of the added noise  $X$ ,  $x_{t+1}$  is the true wind speed in  $t+1$ ,  $y_{t+1}$  is the forecasted wind speed at  $t+1$ , and  $y_t$  is the prediction in  $t$ .

Note that the expected forecasting accuracy will depend on the weather forecasting model used, thus the desired forecasting accuracy of the generated synthetic forecasts in this study will be within the range of the current advanced methods shown in Pathak et al. (2022) and Ben-Bouallegue et al. (2022). The root mean square error (RMSE), defined in equation 4.3, for the obtained forecasts for 2022 can be seen in section 5.1.

$$\text{RMSE} = \sqrt{\frac{1}{n} \sum_{i=1}^n (y_i - \hat{y}_i)^2} \quad (4.3)$$

An example forecast for day 3 and 21 can be seen in figure 4.5. Due to the nature of the synthetic forecasting using an attraction factor, it does not capture the sudden peaks for day 21 seen in figure 4.5.

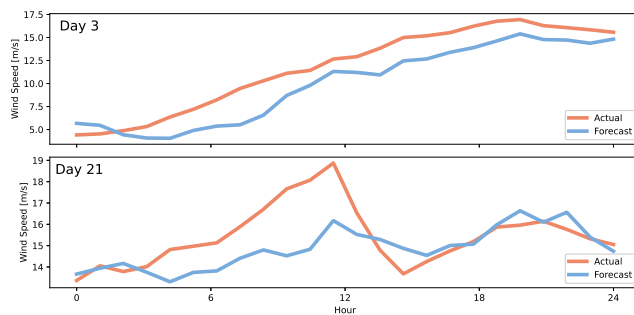


Figure 4.5: Examples of forecasts for day 3 and 21 in 2021.

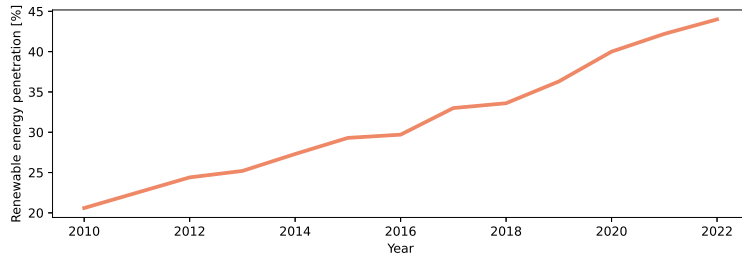


Figure 4.6: Danish Energy Penetration 2010-2022 (Danmarks Statistik)

## Power market forecast

In this section the power market price forecasting methodology will be presented and discussed. Forecasting the electricity market spot prices in an accurate manner provides a better foundation for improving and reducing the O&M costs of operating an OWF. Specifically identifying periods of low prices and placing maintenance in these periods should allow for reduction in the lost revenue due to turbine shutdown during maintenance.

### Forecasting framework

The proposed model uses an iterative framework where the power market forecast is created on a daily basis to provide a forecast for the following day. This provides a 96 hour forecasts which will be used in the O&M decision-making strategy. The forecast will use historical data from the Danish electricity zone DK2 in the period 2019-2021 as training data. Note that the forecasts for 2021 do not include 2021 as a training dataset. The period is chosen due to recency, which is important given the larger penetration of renewable energy sources in recent years, which can have a large impact on the electricity price. The renewable energy penetration in the Danish grid is seen in figure 4.6. As explained in section 4.2 2023 is not used since weather data is partly unavailable for 2023 at the time of data collection.

This study will target medium term forecasting, which has seen the best results in other literature using ANN or statistical approaches. In this study several forecasting methods will be used; a combination of long short-term memory (LSTM) and extreme gradient boost (ANN-XGBoost) from now on referred to as ANN, an Auto-Regressive Integration Moving Average with Exogenous variables (ARIMAX) forecaster and finally an exponentially weighted moving average (EWMA).

### Input data

Besides the historical price data to be used in the model, other input data will be available for the ANN and ARIMAX models. This includes calendar pointers, such as binary variables indicating weekends, seasonality and peak hours during the day. The forecasted wind speed will also be used as input data for the power market models. As seen in figure 4.7 there is a significant negative correlation between wind speeds and the electricity price

in the DK2 electricity zone. There seems to be a strong trend between very high wind speeds and low prices. Thus it is expected that an accurate weather forecast can provide an indication of future prices.

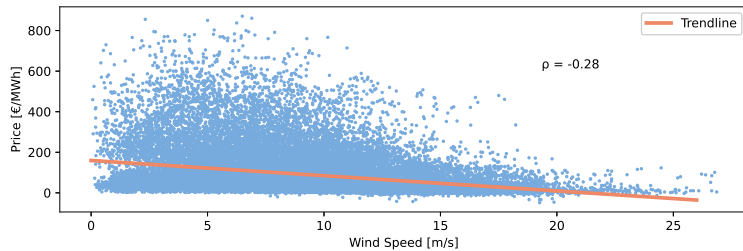


Figure 4.7: Wind speed and Market Clearing price

## ANN

The ANN model is a combination of a LSTM and XGBoost model. The LSTM model is an artificial neural network that is typically used to forecast time series given its ability to remember both long and short term connections in the data (Lindemann et al. 2021). The XGBoost model trains a series of sequential decision trees that aims to correct the residual error of the last tree. The XGBoost model is a standard machine learning library as is introduced in Chen and Guestrin (2016). The LSTM model forecasts the initial prices based on lagged prices, calendar pointers and wind forecasts. Hereafter the XGBoost model is trained to predict the price based on the LSTM output and the initial feature variables resulting in a forecast of future prices. Theoretically the combination of the two models should be more accurate than the predictions given solely by the LSTM model. Note that the prices and wind speeds are normalized, and must be inversely transformed before being used. The overall workflow of the ANN-XGBoost is illustrated in figure 4.8.

To see the full description of the layers in the ANN model, refer to table A.1 in the appendix, and table 4.3 for the XGBoost model training parameters, where the best fit is marked in bold.

The ANN forecasting model uses RMSE as the loss function, and aims to minimize this.

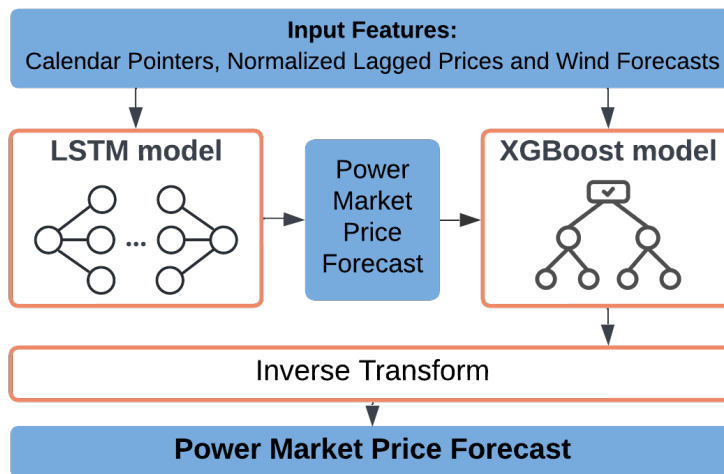


Figure 4.8: Model used to forecast electricity prices. For exact LSTM model parameters see appendix A.1. XGBoost model parameters are shown in table 4.3.

Table 4.3: Fitting Parameters of the XGBoost Model. Best fitting parameters are marked in **bold**.

Parameter	Values	Description
n_estimators	100, 200, <b>300</b>	Number of boosting rounds
learning_rate	0.01, 0.05, <b>0.1</b>	Step size shrinkage to prevent overfitting
max_depth	<b>3, 5, 7</b>	Maximum depth of a tree
min_child_weight	<b>1, 3, 5</b>	Minimum sum of instance weight needed in a child
subsample	<b>0.6, 0.8, 1.0</b>	Subsample ratio of the training instance
colsample_bytree	0.6, 0.8, <b>1.0</b>	Subsample ratio of columns when constructing each tree
gamma	<b>0, 0.1, 0.2</b>	Minimum loss reduction required to make a further partition on a leaf node

## ARIMAX

The ARIMAX forecasting model will use a similar workflow to the ANN model. Here the same set of input data is provided to the ARIMAX model as exogenous variables. The ARIMAX model is fitted for the entire 2019-2020 period when forecasting in 2021 and 2019-2021 when forecasting in 2022. To determine the optimal fitting parameters for the ARIMAX( $p, d, q$ ) model, the three fitting parameters are swept in the ranges:

$$p \in \{0, 1, 2, 3, 4, 5\} \quad (4.4)$$

$$d \in \{0, 1\} \quad (4.5)$$

$$q \in \{0, 1, 2, 3, 4, 5\} \quad (4.6)$$

Here  $p$  is the auto-regressive (AR) order. The AR order defines the number of included lagged dependent variables, which in the context are the previous prices.  $d$  is the integrative (I) order, which defines the  $d$  number of times that the data has to be differentiated to obtain stationarity. A time series can be considered stationary, when it has no drift. Finally  $q$  is the moving average (MA) order, which defines how many previous forecasting errors are included in the future forecast. For each fit, the corresponding Akaike Information Criterion (AIC) value is computed. The best fitting model will have the lowest AIC value, this is explained in more detail in Cavanaugh and Neath (2019). In equation 4.7 an ARIMA(1,0,1) can be seen, which includes 1 AR order and one MA order.

$$Y_t = c + \phi_1 Y_{t-1} + \theta_1 \epsilon_{t-1} + \epsilon_t \quad (4.7)$$

Where  $Y_t$  is the predicted value given the last observation  $Y_t$  and  $\epsilon_{t-1}$  is the last forecast error. Here  $\phi_1$  and  $\theta_1$  are the relative weights of the two models.

When running the sweep of parameters, the AIC value of the fit is saved and can be seen in table A.1 in the appendix. Here the best parameters for the ARIMAX model are noted to be (5,1,4) with an AIC value of approximately -9625. Thus this combination of parameters is used to forecast prices for 2021 and 2022.

## EWMA

The EWMA model, will use the previous prices for each hour to forecast the next 24 hours of the coming day. Here the formula for the forecasted price is given by equation 4.8.

$$\text{EWMA}_h = \sum_{i=0}^{n-1} \alpha(1 - \alpha)^i \cdot P_{h,n-1-i} \quad (4.8)$$

where  $\text{EWMA}_h$  is the forecasted price for hour  $h$ ,  $n$  is the amount of previous prices for hour  $h$ ,  $\alpha$  is the relative weighing of previous prices and  $P_{h,n-1-i}$  is the price at hour  $h$  for day  $n - 1 - i$ . Note here that  $\alpha$  will be a value between 0 and 1, which indicates how previous prices are weighed. Here small values for  $\alpha$  corresponds to a slow response to recent prices and a relatively equal weight independent of recency, and larger values for  $\alpha$  corresponds to a larger weight of recent measurements.

To determine an appropriate level for  $\alpha$ , different values for  $\alpha$ , from 0 to 1, are used to forecast each hour in 2021 given historic prices from 2019 up to the day before the realized price.

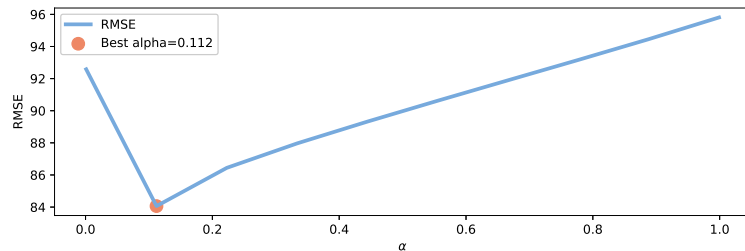


Figure 4.9: RMSE for EWMA with multiple  $\alpha$  values. The optimal value for  $\alpha$  is 0.112.

The RMSE for all  $\alpha$  tested between 0 and 1 are seen in figure 4.9 with the optimal value for  $\alpha$  being 0.112.

## Analysis of forecasting accuracy

To compare the forecasting accuracy across models the RMSE will be used. This is the typical evaluation metric used for comparing power market forecasts as seen in Xiong and Qing (2023).

Due to the rising energy prices throughout 2021 and 2022, as mentioned in section 4.2, the normalized RMSE should allow for a better comparison of forecasting accuracy across time periods with different price levels. It is given by:

$$\text{Normalized RMSE} = \frac{\sqrt{\frac{1}{n} \sum_{i=1}^n (y_i - \hat{y}_i)^2}}{\bar{y}} \quad (4.9)$$

Where  $n$  is the amount of observations,  $y$  are the forecasted values,  $\hat{y}$  are the true values, and  $\bar{y}$  is the average true value in the time period.

## 4.4 O&M Model

The proposed O&M OR model employs various modelling techniques in order to model O&M activities in an OWF. The technique described in Zhang et al. (2017) is used to

model the movement of CTVs between wind turbines, and between the turbines and Klintholm harbour. Here time-space nodes are used to define how vehicle routing can span over several time periods. To allow for more precise scheduling, the problem is defined in 15 minute interval granularity, as opposed to hourly time increments.

## Time-space node approach

One of the challenges of modelling the problem is the different distances between turbines as well as to and from the harbour. Additionally, CTVs should be able to slow down in order to save fuel when going between two nodes. This is achieved by utilizing a time-space node approach. Here each turbine as well as the harbour is represented as nodes. Each node appears once per time step, as in Zhang et al. (2017), here a time step represents 15 minutes. Arcs are generated from each time-space node to future time-space nodes. Computational challenges, that arise due to the number of arcs, are addressed in section 4.4, which discusses the reduction in the number of arcs. In the model, the CTVs are able to travel through the arcs, which will bring them from one node at a given time to another node at a future time. Note that one of the added benefits of this approach is the enabling of the CTVs to travel through longer arcs between nodes, which results in the same distance travelled but at a lower speed. Lower CTV speeds lead to reduced fuel consumption and thereby reduced greenhouse gas (GHG) emissions (Gusti and Semin 2016). This is further discussed in section 4.8.

To keep track of the amount of CTVs used in the model, a virtual node for each CTV in the harbour will be generated. All virtual nodes share the same location in the distance matrix  $D$ . This simplifies the MILP, as the CTVs are prohibited from using the same arcs, and thus a separate path for each CTV is created.

## Maintenance

The model categorizes maintenance into two types. The first category is a catastrophic failure which requires CM in order to be repaired. These failures cause turbine shutdowns and must be prioritized, as power production is halted for the specific turbine until CM is completed. The catastrophic failure will be generated based on the results presented in Carroll, McDonald, and McMillan (2016) where failure types and rates are available. See section 4.4 where the failure types and rates are presented, and the failures used in the simulations are generated.

The second category of maintenance is SM. This is maintenance that has to be done at some point, but does not cause a shutdown of the wind turbine until the repair is taking place. In simulations all turbines start out with the same amount of SM.

This study will not include PM in the scheduling framework. If needed this could poten-

tially be added to the existing SM with a slightly higher weighting in order to get it done before SM.

### Maintenance generation

Maintenance is at the center of this study. A realistic generation of failures is therefore needed. While failure rates are often not readily available from current OWF projects, Carroll, McDonald, and McMillan (2016) has a collection of failure rates used by many other studies as described in the introduction. In the work of Carroll, McDonald, and McMillan (2016) failures are split into sub-assemblies, with a sub-assembly being a part of the turbine such as gearbox or transformer, and a cost-category. Each combination of sub-assembly and cost-category has a specific cost, failure rate and repair time. The failure rate and repair time is directly used in this study, with the failure generation only being done once for the years 2021, and 2022. The costs associated with a repair such as replacement parts are not included, as they cannot be optimized within the framework of this study. The aggregated failure characteristics for 2021 and 2022 is shown in table 4.4. For the generated failures 2022 has more incidents per turbine and overall CM hours.

Table 4.4: Characteristics of generated failures for 2021 & 2022.

	<b>2021</b>	<b>2022</b>
<b>Mean number of failures per Turbine</b>	8.34	8.58
<b>Mean CM hours per failure</b>	13.14	13.99
<b>Mean total CM hours per Turbine</b>	109.57	120.00

The maintenance is generated once per year in order to allow for a more direct comparison between simulations done on the same year.

### Postponement Cost

As SM does not come with a direct cost due to shutdowns like CM, it will not automatically be carried out by the model. To ensure that the model decides to do SM in periods of low forecasted revenue the model is penalized for postponing SM to the next iteration. A postponement cost is added to all quarters of SM that is postponed to the next iteration. The level of this postponement cost determines how aggressive the model is in doing SM. Note that the postponement penalty can either be set as a fixed value or use a quantile of past prices. In section 5.2 simulations will be performed with a range of postponement costs and the impact on the amount of SM performed is investigated. It is important to note that the postponement penalty is purely a modelling parameter, that is only required to model the scheduling of maintenance. It is thus not comparable to other input such as forecasts etc. The postponement cost can however to a certain extend be interpreted as the threshold level of when the model decides that maintenance can be done. Thus a

quarter of maintenance must be cheaper, based on the forecasts as well as fuel costs, to do than the corresponding postponement penalty if it is to be scheduled by the model.

While not performing CM has a direct cost due to lost revenue, there can be cases where the amount of CM on a given turbine is more than what can be repaired before the end of the planning horizon. The model will thus no longer see a benefit by repairing a catastrophic failure, as the turbine will not be able to produce power during the planning horizon. To counteract this issue an extra sufficiently high cost of 1000€ is applied to each quarter of CM that has not been carried out at the end of the planning horizon. The planning horizon is further explained in section 5.2.

## Problem Formulation

The developed model is based on decision variables, parameters and sets. Decision variables are shown in table 4.5, sets are shown in table 4.6, and model parameters are shown in table 4.7.

To maximize the profit of the O&M activities an objective is defined. The objective function will be given by the total expected revenue given the operational status of the wind turbines  $x_{t,w}$ , the forecasted wind speeds  $ws_t$ , the power curve  $\Theta_w$  and the forecasted prices  $p_t$ .  $\Theta_w(WS_t)$  is thereby the amount of power produced by turbine  $w$  in quarter  $t$ . The maintenance costs  $MC_t$  and postponement penalty  $PP$  are subtracted the revenue from sold electricity.

Objective function:

$$\max \left\{ \sum_{\forall t \in T} \sum_{\forall w \in W} x_{t,w} \cdot \Theta_w(ws_t) \cdot p_t - MC_t - PP \right\} \quad (4.10)$$

The realized profit  $\Pi$  from the operation of the wind farm will be given by the revenue from the sale of power and the maintenance costs. The revenue from the sale of power will be given by the realized prices, wind speeds and operational status. The maintenance costs will be the same as derived from the optimization model:

$$\Pi = \sum_{\forall t \in T} \sum_{\forall w \in W} x_{t,w} \cdot \Theta_w(WS_t) \cdot \pi_t - MC_t \quad (4.11)$$

Here  $x_{t,w}$  is the operational status of turbines  $w$  at time  $t$ ,  $\Theta_w(WS_t)$  is the realized power production of turbine  $w$  in quarter  $t$  given its power curve  $\Theta_w$  and the wind speed  $WS_t$  with the unit  $MWh$ , and the realized day-ahead price  $\pi_t$  at quarter  $t$ .

For a complete unit check of the model, see appendix section A.2.

Table 4.5: Decision variables used in the model.

Decision variables		
Symbol	Unit	Explanation
$x_{t,w}$	-	Binary variable stating whether a wind turbine is shut down.
$MC_t$	€	Maintenance cost for each quarter.
$PP$	€	Postponement penalty.
$r_{t,w}^{CM}$	-	Binary variable indicating whether a certain quarter $t$ , has CM being performed on wind turbine $w$ .
$r_{t,w}^{SM}$	-	Binary variable indicating whether a certain quarter $t$ , has a SM being performed on wind turbine $w$ .
$h_{t,w}^{CM}$	Quarters	Total quarters of CM needed at time $t$ on turbine $w$ before being operational.
$h_{t,w}^{SM}$	Quarters	Total quarters of SM needed at time $t$ on turbine $w$ .
$Z_{i,t,w}$	-	Binary variable equal to one if CTV $i$ is at turbine $w$ at time $t$ .
$MS_{t,w}^{CM}$	-	Binary variable denoting the start of CM for turbine $w$ at time $t$ .
$MS_{t,w}^{SM}$	-	Binary variable denoting the start of SM for turbine $w$ at time $t$ .
$ME_{t,w}^{CM}$	-	Binary variable denoting the end of CM for turbine $w$ at time $t$ .
$ME_{t,w}^{SM}$	-	Binary variable denoting the end of SM for turbine $w$ at time $t$ .
$MS_{t,w}$	-	Binary variable denoting if any maintenance at turbine $w$ starts at quarter $t$ .
$ME_{t,w}$	-	Binary variable denoting if any maintenance at turbine $w$ ends at quarter $t$ .
$A_{s,t,r,t'}$	-	Set of all arcs flowing from time space node $s, t$ into $r, t'$ .

Table 4.6: Sets used in the model

Sets	
Symbol	Explanation
$O$	Set of quarters between 20:00 and 8:00 where maintenance cannot be done.
$W$	Set of wind turbines.
CTV	Set of CTVs available.
$T$	Set of quarters throughout the planning period. 96 quarters if planning horizon is one day, see section 5.2.
$N$	Set of all nodes including turbine and CTV harbour nodes.

Table 4.7: Input parameters used in the model.

## Parameters

Symbol	Unit	Explanation
$W^{\#}$	-	Number of turbines.
CREW	-	Number of crews.
CCC	-	CTV crew capacity.
$CTV^{\#}$	-	Number of CTVs.
$ws_t$	m/s	Wind speed forecast at quarter $\forall t \in T$ .
$WS_t$	m/s	Realized wind speed at quarter $\forall t \in T$ .
$wh_t$	m	Significant wave height forecast at quarter $\forall t \in T$
WHL	m	Maximum wave height. If surpassed CTVs have to be in harbour and no maintenance can be performed.
WSL	m/s	Maximum wind speed. If surpassed CTVs have to be in harbour and no maintenance can be performed.
$\Theta_w(ws_t)$	MWh	Power production for wind turbine $w$ and wind speed $ws_t$ at time $t$ .
$p_t$	$\frac{\text{€}}{\text{MWh}}$	Forecast spot price for $t$ .
$\pi_t$	$\frac{\text{€}}{\text{MWh}}$	Realized spot price for $t$ .
$PP_{cost}^{SM}$	€/Hour	Cost of postponing one hour of SM beyond the planning horizon.
$PP_{cost}^{CM}$	€/Hour	Cost of postponing one hour of CM beyond the planning horizon. Fixed to 4000€/Hour.
$FC$	€/L	Fuel cost per liter for the CTVs.
$D_{s,r}$	m	Distance between two nodes, $s$ and $r$ , for nodes $\in N$ .
$H_w^{SM}$	Quarters	Amount of SM needed for turbine $w$ at $t = 1$ .
$H_w^{CM}$	Quarters	Amount of CM needed for turbine $w$ at $t = 1$ .
$\delta$	Quarters	Number of quarters the arcs go forward in time (Arc lookout time).
$M_{cm}$	Quarters	Big M for shutdown of turbines with remaining CM.
$M_{wh\_limit}$	m	Big M for WHL.
$M_{ws\_limit}$	m/s	Big M for WSL.

## Constraints

In addition to the objective function constraints are used to define the problem and model the O&M activities described previously.

$$MC_t = FC \sum_{\substack{(s,r) \in N \\ t'=1:t+\delta}} C_{s,r,t'-t} \cdot A_{s,t,r,t'} \quad \forall t \in T \quad (4.12)$$

$$h_{t,w}^{CM} \leq (1 - x_{t,w}) \cdot M_{cm} \quad \forall t \in T, \forall w \in W \quad (4.13)$$

$$h_{1,w}^{CM} = H_w^{CM} - r_{1,w}^{CM} \quad \forall w \in W \quad (4.14)$$

$$h_{1,w}^{SM} = H_w^{SM} - r_{1,w}^{SM} \quad \forall w \in W \quad (4.15)$$

$$h_{t+1,w}^{CM} = h_{t,w}^{CM} - r_{t,w}^{CM} \quad \forall t \in \{1, \dots, |T| - 1\}, \forall w \in W \quad (4.16)$$

$$h_{t+1,w}^{SM} = h_{t,w}^{SM} - r_{t,w}^{SM} \quad \forall t \in \{1, \dots, |T| - 1\}, \forall w \in W \quad (4.17)$$

$$(1 - r_{t,w}^{CM}) \geq x_{t,w} \quad \forall t \in T, \forall w \in W \quad (4.18)$$

$$(1 - r_{t,w}^{SM}) \geq x_{t,w} \quad \forall t \in T, \forall w \in W \quad (4.19)$$

$$MS_{t,w}^{SM} \geq r_{t,w}^{SM} - r_{t-1,w}^{SM} \quad \forall t \in \{2, \dots, |T|\}, \forall w \in W \quad (4.20)$$

$$ME_{t,w}^{SM} \geq r_{t,w}^{SM} - r_{t+1,w}^{SM} \quad \forall t \in \{1, \dots, |T| - 1\}, \forall w \in W \quad (4.21)$$

$$MS_{t,w}^{CM} \geq r_{t,w}^{CM} - r_{t-1,w}^{CM} \quad \forall t \in \{2, \dots, |T|\}, \forall w \in W \quad (4.22)$$

$$ME_{t,w}^{CM} \geq r_{t,w}^{CM} - r_{t+1,w}^{CM} \quad \forall t \in \{1, \dots, |T| - 1\}, \forall w \in W \quad (4.23)$$

$$r_{t,w}^{SM} + r_{t,w}^{CM} \leq 1 \quad \forall t \in T, \forall w \in W \quad (4.24)$$

$$2 \cdot MS_{t,w} \geq MS_{t,w}^{CM} + MS_{t,w}^{SM} \quad \forall t \in T, \forall w \in W \quad (4.25)$$

$$2 \cdot ME_{t,w} \geq ME_{t,w}^{CM} + ME_{t,w}^{SM} \quad \forall t \in T, \forall w \in W \quad (4.26)$$

$$\sum_{ctv \in CTV} Z_{ctv,t,w} \geq MS_{t,w} \quad \forall t \in T, \forall w \in W \quad (4.27)$$

$$\sum_{ctv \in CTV} Z_{ctv,t,w} \geq ME_{t,w} \quad \forall t \in T, \forall w \in W \quad (4.28)$$

$$wh_t \leq WHL + M_{wh\_limit} \cdot Z_{ctv,t,W^{\#}+ctv} \quad \forall t \in T, \forall ctv \in CTV \quad (4.29)$$

$$wh_t \leq WHL + M_{wh\_limit} \cdot (1 - \sum_{w \in W} r_{t,w}^{SM} + r_{t,w}^{CM}) \quad \forall t \in T \quad (4.30)$$

$$ws_t \leq WSL + M_{ws\_limit} \cdot Z_{ctv,t,W^{\#}+ctv} \quad \forall t \in T, \forall ctv \in CTV \quad (4.31)$$

$$ws_t \leq WSL + M_{ws\_limit} \cdot (1 - \sum_{w \in W} r_{t,w}^{SM} + r_{t,w}^{CM}) \quad \forall t \in T \quad (4.32)$$

$$r_{t,w}^{SM} = r_{t,w}^{CM} = 0 \quad \forall t \in O \quad (4.33)$$

$$r_{t,w}^{SM} = r_{t,w}^{CM} = 0 \quad \forall t \in O \quad (4.34)$$

$$Z_{ctv,t,w} = 1 \quad \forall ctv \in CTV, \forall t \in O, \forall w \in \{W^{\#} + ctv\} \quad (4.35)$$

$$PP = \sum_{w \in W} h_{|T|, w}^{SM} \cdot \frac{PP_{cost}^{SM}}{4} + h_{|T|, w}^{CM} \cdot \frac{PP_{cost}^{CM}}{4} \quad (4.36)$$

$$\sum_{\substack{r \in N \\ t' = t - \delta : t - 1}} A_{r, t', s, t} = \sum_{\substack{r \in N \\ t' = t + 1 : t + \delta}} A_{s, t, r, t'} \quad \forall t \in \{\delta + 1, \dots, |T| - \delta\}, s \in N \quad (4.37)$$

$$\sum_{\substack{r \in N \\ t' = 1 : t - 1}} A_{r, t', s, t} = \sum_{\substack{r \in N \\ t' = t + 1 : t + \delta}} A_{s, t, r, t'} \quad \forall t \in \{2, \dots, \delta + 1\}, s \in N \quad (4.38)$$

$$A_{s, t, r, t'} \leq \max(0, (t' - t) - Ds, r) \quad \forall s, \forall r \in N, \\ \forall t \in \{1, \dots, |T| - \delta\}, \\ \forall t' \in \{t + 1, \dots, t + \delta\} \quad (4.39)$$

$$\sum_{\substack{(s, r) \in N \\ t' = 2 : 1 + \delta}} A_{s, t, r, t'} = CTV^\# \quad t = 1 \quad (4.40)$$

$$\sum_{\substack{r \in N \\ t' = t + 1 : t + \delta}} A_{s, t, r, t'} \leq 1 \quad \forall t \in \{1, \dots, |T| - \delta\}, s \in N \quad (4.41)$$

$$\sum_{\substack{s \in N \\ t = t' - \delta : t' - 1}} A_{s, t, r, t'} = \sum_{ctv \in CTV} Z_{ctv, t', r} \quad \forall r \in N, \forall t' \in \{1 + \delta, \dots, |T|\} \quad (4.42)$$

$$\sum_{\substack{s \in N \\ t = 1 : t' - 1}} A_{s, t, r, t'} = \sum_{ctv \in CTV} Z_{ctv, t', r} \quad \forall r \in N, \forall t' \in \{2, \dots, \delta\} \quad (4.43)$$

$$A_{s, t, r, t'} + Z_{ctv, t, s} \leq Z_{ctv, t', r} + 1 \quad \forall t \in \{1, \dots, |T| - \delta\}, \\ \forall t' \in \{t + 1, \dots, t + \delta\}, \\ \forall s, \forall r \in N, \forall ctv \in CTV \quad (4.44)$$

$$\sum_{ctv \in CTV} crew_{t, ctv} \leq CREW \quad \forall t \in T \quad (4.45)$$

$$crew_{t, ctv} \leq CCC \quad \forall t \in T, \forall ctv \in CTV \quad (4.46)$$

$$Z_{ctv, t, w} + MS_{t, w} - 1 \leq crew_{t-1, ctv} - crew_{t, ctv} \quad \forall t \in \{2, \dots, |T|\}, \\ \forall w \in W, \forall ctv \in CTV \quad (4.47)$$

$$Z_{ctv, t, w} + ME_{t, w} - 1 \leq crew_{t+1, ctv} - crew_{t, ctv} \quad \forall t \in \{1, \dots, |T| - 1\}, \\ \forall w \in W, \forall ctv \in CTV \quad (4.48)$$

$$\sum_{\forall w \in W} r_{t, w}^{SM} + r_{t, w}^{CM} + \sum_{\forall ctv \in CTV} crew_{t, ctv} = CREW \quad \forall t \in T \quad (4.49)$$

$$\sum_{\forall ctv \in CTV} Z_{ctv, t, w} \leq 1 \quad \forall t \in T, \forall w \in W \quad (4.50)$$

$$\sum_{\substack{t=1:T, \\ ctv'=1:CTV, ctv'!=ctv}} Z_{ctv, t, W + ctv'} = 0 \quad \forall ctv \in CTV \quad (4.51)$$

In eq. (4.12) the fuel cost of the CTVs is computed by summing over the arcs used in the model  $A$  and the associated fuel consumption of travelling along the arc  $C_{s,r,t'-t}$  multiplied by the fuel cost  $FC$ . The model uses a fuel cost of 0.25 €/L which is a price of marine fuel seen at the start of 2021 (Jordan and Lasek n.d.). Equation (4.13) ensures that turbine  $w$  at time  $t$  cannot generate power, if any CM remains. In eq. (4.13) the 'big M' notation is used where  $M_{cm}$  is set to be the maximum amount of remaining maintenance that a wind turbine should experience. In this study  $M_{cm}$  is set to 5 times the largest fault of 298 hours:

$$M_{cm} = 5 \cdot 4 \cdot \frac{[\text{quarters}]}{[\text{hours}]} \cdot 298 [\text{hours}] = 5,960 \quad (4.52)$$

In eqs. (4.16) and (4.17) the remaining amount of time for CM and SM is updated and reduced if maintenance has taken place. Equations (4.18) and (4.19) ensure that the wind turbines do not run while repairs are taking place for turbine  $w$  and time  $t$ . Equations (4.20) to (4.23) forces the variables  $MS_{t,w}^{SM}$ ,  $ME_{t,w}^{SM}$ ,  $MS_{t,w}^{CM}$  and  $ME_{t,w}^{CM}$  to be active, when a change in repair happens. In eqs. (4.25) to (4.28) the scheduled and catastrophic repairs are bundled together to ensure that a CTV must be present in time-space node  $(t, w)$  if maintenance is to be started or ended.

In eqs. (4.29) to (4.32) the CTVs must be in harbour and no maintenance can be performed if the forecasted wind speed  $ws_t$  or wave height  $wh_t$  are higher than the corresponding WHL or WSL. Equations (4.33) to (4.35) ensures than no maintenance takes place in closed hours, when  $t \in O$ . In eq. (4.36) the postponement penalty is defined as the sum of remaining CM and SM that has not been done at time  $|T|$  multiplied by their respective postponement penalty. Not forcing the mode to perform a certain amount of SM allows the model to postpone SM if the forecasted revenue is extraordinarily high. Note that the price factor  $PP_{cost}$  is divided by four to cater for the quarterly granularity.

In eqs. (4.37) to (4.41) the arcs from time-space node  $(s, t)$  to  $(r, t')$  are constrained. The constraint in eq. (4.37) ensures that sum of used arcs entering node  $(s, t)$  is equal to the sum of used outgoing arcs. This ensures that a CTV cannot exit from a node if it did not enter the time-space node in the previous time-step. Note here that a CTV must use an arc even when remaining stationary in a node. Equation 4.38 is the corner case of equation 4.37, but is slightly altered to cater for the arc lookout period  $\delta$ . To incorporate the actual travel time between nodes equation 4.39 is used. This ensures that arcs can only be used if the arc length in quarters is greater than the corresponding minimum time

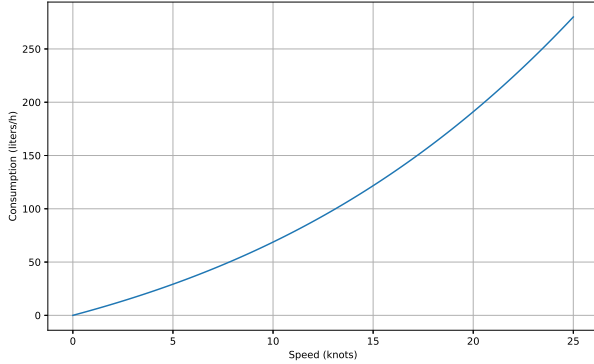


Figure 4.10: Fuel consumption profile of a CTV as a function of speed

needed to go between two nodes defined in the distance time matrix. That the sum of CTVs that can exit the first time-space nodes, which in this context is Klintholm harbour, should be equal to the number of CTVs ( $CTV^{\#}$ ) is defined in eq. (4.40). In equation 4.41 the number of arcs leaving a specific time-space node is limited to at most one. Note here that as mentioned in section 4.4 each CTV has a virtual node in the harbour. In equations 4.42 and 4.43 the sum of arcs traveling into node  $r, t'$  must be equal to the sum of CTVs in the node, thus an arc cannot be active without a CTV using the arc. Equation 4.44 tracks each CTV individually. The allocation of crew to and from the harbour is handled in eqs. (4.45) to (4.49). Here the total amount of crews across the CTVs as well as the turbines is given in eqs. (4.45) and (4.49). In eq. (4.46) the maximum amount of crews that each CTV can carry is given by  $CCC$ . Equations (4.47) and (4.48) updates the amount of crew on each CTV as maintenance is either started or stopped. Equation 4.50 ensures that only one CTV can be at one time-space node. Finally equation 4.51 makes sure that each CTV does not use any of the other CTVs' harbour nodes.

## Derivation of distance and consumption matrix

A key feature of the time-space node approach is its ability to choose between routes with varying travel times. This effectively results in a slower travel speed between nodes. Slower travel speeds between nodes lead to reduced fuel consumption, thereby saving costs and reducing CO<sub>2</sub> emissions. Fuel consumption relative to travel speed is determined using the specifications of the consumption profile of a relevant CTV. Here the consumption for a comparable CTV in size and speed is used. According to *Windcat 42 / FRS Windcat Offshore Logistics* (n.d.), the fuel consumption is 280 liters per hour at 25 knots, this is also considered the maximum speed and thus the maximum consumption. Combining this with the power curve from Meyer, Stahlbock, and Voss (2012) fuel consumption decreases by approximately 66% when the speed is halved. This relationship is fitted using a third-degree polynomial, resulting in the consumption curve shown in Figure 4.10.

The distance matrix ( $D$ ) is derived from the physical layout discussed in section 4.1,

where  $D_{i,j}$  indicates the minimum travel time in quarters between wind turbines  $i$  and  $j$ . Additionally in  $D$  the last  $CTV^{\#}$  of rows and columns contains the distance from the wind turbines back to each virtual CTV harbour. For instance if  $D_{i,j} = 3$  it takes at least 3 quarters for the CTV to travel from node  $i$  to  $j$ .

This method approximates the consumption at different speeds for CTVs employed at Kriegers Flak. In a real-life application, the exact consumption profile would be known and directly implemented. The consumption matrix is then given by:

$$C_{i,j,t} = \frac{t}{4} \cdot CP \left( \frac{D_{i,j}}{\frac{t}{4}} \right) \quad (4.53)$$

Where  $C_{i,j,t}$  represents the consumption of fuel (in liters) for travelling from node  $i$  to  $j$  using  $t$  time steps.  $D_{i,j}$  is the distance from node  $i$  to  $j$ , and  $CP$  is the consumption profile.

## Assumptions in the model

In the model there are several assumptions that simplify the model. The most important assumptions are listed here.

**Interchangeable Crew:** It is assumed that any crew can carry out any kind of maintenance both CM and SM.

**Interchangeable CTVs:** It is assumed that all maintenance can be carried out by all CTVs. Even large maintenance tasks such as gearbox or wind blade change can be carried out by a CTV given enough maintenance hours.

**Drop off times:** It is assumed that the drop off times are negligible. The drop off times in this context is the transfer period that occur when a CTV has arrived at an OWT and the crew transfers to the OWT. It should be noted that all travel times are rounded up to the nearest quarter giving some leeway to drop off crews. To include more drop off time an extra time step could be added to equation 4.39 and changing the time index for the consumption matrix in equation 4.12.

**Lack of HSE rule:** The health safety and environment (HSE) rule that states that a CTV must be within 20 minutes of crews performing maintenance is not implemented.

## Computational Complexity

To keep the computational complexity of the model low is it essential to keep the number of variables low. However, when applying the time-space node approach a large number of arcs and thereby variables are generated. Using a forecasting horizon of 96 hours in a quarterly granularity and 73 nodes (72 turbines and 1 harbour) the amount of arcs is calculated by:

$$N * (N - 1) = 24 \cdot 4 \cdot 74 \cdot (24 \cdot 4 \cdot 74 - 1) = 807,649,440 \quad (4.54)$$

Here there are various methods of minimizing the number of arcs and thus the computational complexity of the model. The most significant improvement that can be made without sacrificing optimality by removing arcs that travel backwards in time as in eq. (4.55):

$$(s, t) \rightarrow (r, t'), t' < t \quad (4.55)$$

This effectively removes half of all arcs. There are also other improvements to be made here such as the closure of arcs between wind turbines during closed hours. Here the CTVs are forced to stay in the harbour and thus any other arcs cannot be utilized. This can be done by implementing the following constraints:

$$A_{s,t,r,t'} = 0 \quad \forall s \in N, \forall r \in W, \forall t \in O, \forall t' \in \{t + 1, \dots, t + \delta\} \quad (4.56)$$

$$A_{s,t,r,t'} = 0 \quad \forall s \in W, \forall r \in N, \forall t \in O, \forall t' \in \{t + 1, \dots, t + \delta\} \quad (4.57)$$

This will allow the solver to immediately remove these arcs from a potential solution and thus reducing the solution space significantly. Additionally, all of the decision variables regarding maintenance can be set to zero during night hours.

$$MS_{t,w} = 0 \quad \forall t \in O, \forall w \in W \quad (4.58)$$

$$ME_{t,w} = 0 \quad \forall t \in O, \forall w \in W \quad (4.59)$$

$$MS_{t,w}^{CM} = 0 \quad \forall t \in O, \forall w \in W \quad (4.60)$$

$$ME_{t,w}^{CM} = 0 \quad \forall t \in O, \forall w \in W \quad (4.61)$$

$$MS_{t,w}^{SM} = 0 \quad \forall t \in O, \forall w \in W \quad (4.62)$$

$$ME_{t,w}^{SM} = 0 \quad \forall t \in O, \forall w \in W \quad (4.63)$$

To further reduce the computational complexity of the model, arcs are only generated from time-space node  $(s, r)$  to time-space nodes  $(\delta)$  time steps into the future. This limits the length of the arcs and thus the maximum amount of travel time between nodes. A natural maximum value for  $\delta$  would be equal to the longest possible arc that a CTV could take during the day, which would logically make sense. In this context this value would be 10 hours or 40 time periods (quarters), as a CTV could quickly travel to one of the

nearest wind turbines and then take the slowest route back to harbour. This value of  $\delta$  does however not significantly reduce the number of arcs, so a smaller value must be used. The amount of arcs generated increases exponentially with the arc lookout period  $\delta$ . To determine an appropriate value for  $\delta$  the model will be run with a varying value for  $\delta$ , where the trade off between computational efficiency and diminishing returns of the objective value is investigated.

The amount of arcs generated given a planning horizon  $T$  can be computed using the two formulas:

$$A_{before} = 74^2 \cdot 4^2 \cdot T^2 \quad (4.64)$$

$$A_{after} = 74^2 \cdot 4^2 \cdot T \cdot \delta \quad (4.65)$$

Here it can be seen that the amount of arcs before the additional measures exponentially increase with  $T$ , but after the implementation of  $\delta$ , the amount of arcs is linearly increasing with  $T$ . For a planning horizon of 1 day (96 quarter) the method creates a 16 fold reduction in the number of generated arcs. The difference in the number of arcs with an increasing planning horizon can be seen in figure 4.11.

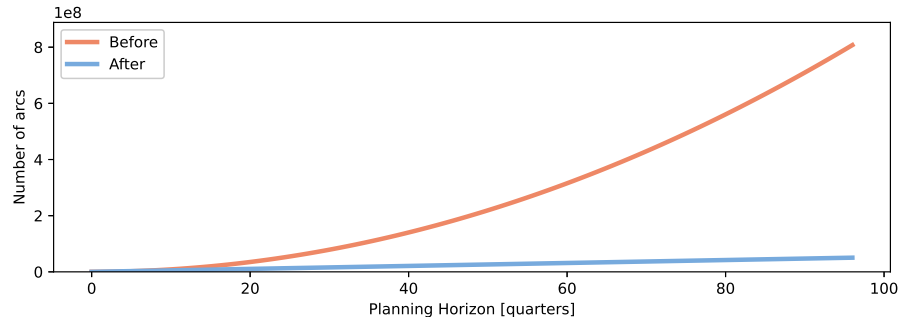


Figure 4.11: Amount of arcs before and reducing amount of arcs as a function of planning horizon ( $T$ ) for  $\delta = 6$ . For a planning horizon of 1 day (96 quarters) the original amount of arcs is 16 times higher than after reducing the number of arcs.

## Matheuristic approach

An additional method of simplifying the problem is to define a matheuristic that can narrow down the problem and the solution space. The matheuristic will be defined as follows. If any CM remains to be done on any wind turbine, a group of the closest  $n$  turbines with remaining SM surrounding the turbine with the most amount remaining CM is created, the group of turbines is also referred to as a cluster later in this study. Only these  $n$  turbines can be visited along with any other turbine with remaining CM. If no CM remains to be done, then the first  $n$  turbines are available given the ordering as seen in figure 4.12A. The matheuristic is shown in pseudo code in algorithm 1.

---

**Algorithm 1** Reduction of model size/complexity heuristic

---

```

 $Openturbines \leftarrow \emptyset$ 
if  $\sum h_{0,w}^{CM} > 0$  then
     $i \leftarrow \arg \max_w (h_{0,w}^{CM})$ 
     $indices \leftarrow argsort(D_{i,w})$ 
    for  $j \in indices$  do
        if  $|Openturbines| = n$  then
            break
        else  $h_{0,j}^{SM} > 0$ 
             $OpenTurbines \leftarrow OpenTurbines \cup \{j\}$ 
     $OpenTurbines \leftarrow OpenTurbines \cup g$  where  $h_{0,g}^{CM} > 0$ 
    else
        for  $i = 1$  To  $W$  do
            if  $|Openturbines| = n$  then
                break
            else
                if  $h_{0,j}^{SM} > 0$  then
                     $OpenTurbines \leftarrow OpenTurbines \cup \{j\}$ 
                else
                    continue

```

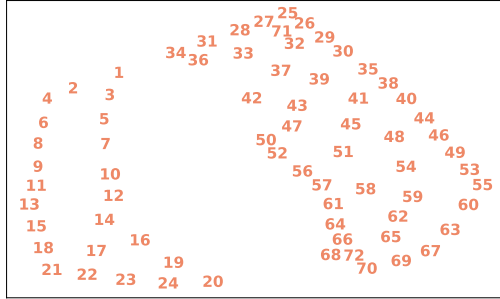
---

To implement the heuristic the following constraints are enforced:

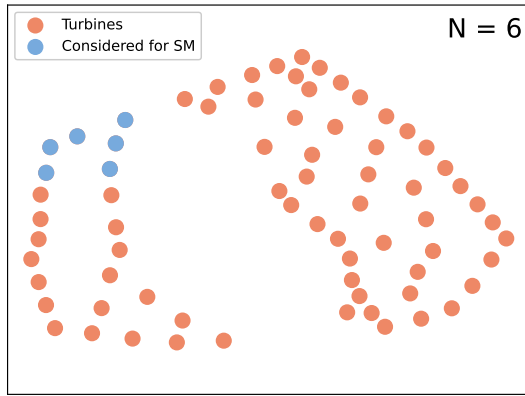
$$Z_{[ctv,t,w]} = 0 \quad \forall t \in T, \forall ctv \in CTV, \forall w \notin OpenTurbines \quad (4.66)$$

$$MS_{[t,w]} = 0 \quad \forall t \in T, \forall w \notin OpenTurbines \quad (4.67)$$

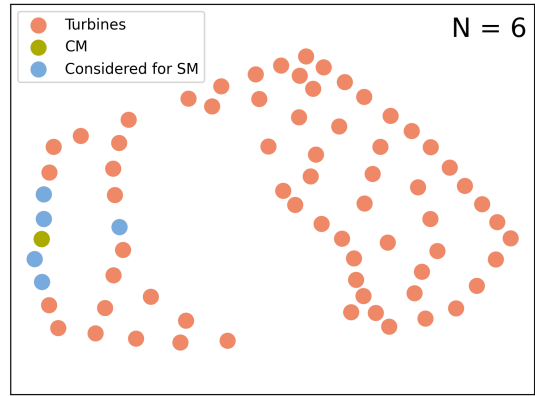
$$ME_{[t,w]} = 0 \quad \forall t \in T, \forall w \notin OpenTurbines \quad (4.68)$$



(A) The turbine numbering used in the heuristic approach.



(B) Heuristic when no CM exists.



(C) Heuristic when CM exists.

Figure 4.12: Turbine numbering and heuristic visualized with the heuristic parameter set to 6 turbines considered for maintenance. Note that the turbine with CM is also considered for SM, however not at the same time.

This heuristic reduces the amount of time-space nodes to only consider the most relevant wind turbines. It is expected that the computational time will decrease with lower values of  $n$ , however also followed by a decrease in the objective value. The change in computational speed and objective value is investigated in section 5.2.

In figure 4.12 the heuristic approach is visualized for two cases. In figure A no CM remains to be done and thus only SM is considered. In figure B there exists CM and thus the OWTs closest the OWT with CM are selected.

## 4.5 Computation - High Performance Compute

As described in section 4.4, the OR model scales to a large size as the number of turbines get larger and thereby increasing the memory load and solve time. All demanding simulations are computed at DTU High Performance Compute (HPC) on a Lenovo ThinkSystem SD530 configured with an Intel Xeon Gold 6226R using 16 cores with 64 GB of RAM (Technical University of Denmark 2024). Having access to the large amount of RAM is

essential to running the model with many turbines in reasonable time as seen in figure 5.9B in the results section.

## 4.6 Analysis of model

To analyze the performance and decision making of the model both short-term and long-term decision will be evaluated.

### Short term simulations - Case study

To evaluate how the model makes decisions based on the revenue forecasts available to the model case studies for single days are carried out. This enables validation of CTV routes and crew placements. The case studies can be seen in section 5.4, where results of running the O&M model are presented.

### Long term simulations

Running the optimization model recurringly for each day enables the model to perform long-term simulations of the O&M activities. For each day the day-specific constraints are updated to reflect the past decisions and the new state of the OWF. The recursive method is illustrated in figure 4.13.

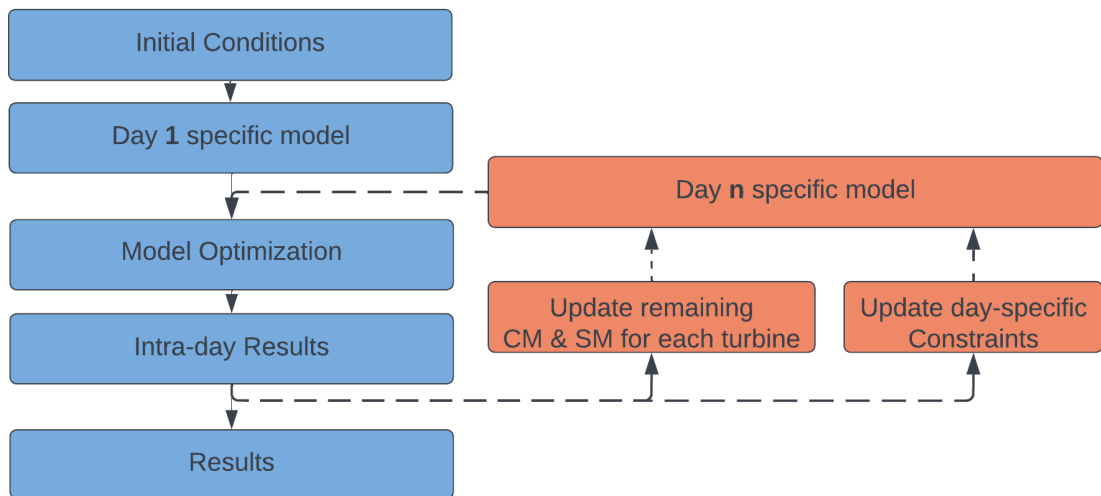


Figure 4.13: Flowchart of the model architecture. The orange part represents the iterative process of updating and running the model for each day,  $n$ , based on the initial model created for day 1. The update of day-specific constraints is further explained in section: Model architecture.

### Model architecture

As discussed in 4.4 the number of variables becomes very large as the model scales. Because of this the time it takes to define the model also becomes increasingly large. It is therefore essential to minimize amount of constraints needed to be redefined between each recursive model run.

When completely defining a model with 36 turbines, 1 CTV, 4 CREW, a planning horizon of 1 day, and no matheuristic applied, the number of constraints is: 3,194,332. However the number of constraints that are specific to a certain day is: 10,825, which is only 0.3% of the total number of constraints.

To optimize the performance of the model, the model is not completely redefined between each day. Here only day-specific constraints are deleted and redefined. This can be seen in figure 4.13. The constraints that are updated between each run are: equations 4.29, and 4.31 since the WHL and WSL are not enforced at the same times from day to day. Equation 4.36 since the PP cost can be different from day to day if a quantile defined PP cost, as described in section 4.4, is used. Equations 4.14 and 4.15 defines the amount of CM and SM at the start of each day, and therefore these also have to be redefined. Apart from these constraints, the heuristic constraints that limit the size of the model and select a set of turbines, as described in section 1 and shown in eqs. (4.66) to (4.68), are also redefined for each day. Only redefining the day-specific part of the model creates a 91% reduction in running times. The model definition and solving times for the optimized model are illustrated in section 5.3.

Another computational efficiency gain of only redefining the day-specific constraint is a warm start based on the previous day solution. As the amount of maintenance left can change from day to day, a warm start only produces a feasible solution if no maintenance has been done in the previous day, so that equations 4.14 and 4.15 are the same from day to day.

## 4.7 Methods Compared

To establish the performance of the opportunistic methods it is essential to have a base case to compare with. The absolute numeric output of the model can be difficult to interpret and compare to other studies due to differences in model parameters, assumptions, and values. Therefore the results are compared to other methods based on the same OR model developed in this study. Overall the methods can be categorised in three categories: Revenue-based opportunistic, Production-based opportunistic, and NAIVE methods. The models that will be compared in this project are:

### PERFECT

The PERFECT method has perfect knowledge of future day-ahead prices. It combines this with the non-perfect weather forecast to obtain a revenue forecast. Maintenance is scheduled based on this revenue forecast. This is expected to be the best performing method.

## ANN

The ANN method uses the LSTM and XGBoost model combination to forecast energy market prices, as discussed in section 4.3. Together with the weather forecast a revenue forecast is created and used to schedule maintenance.

## EWMA

The EWMA method uses an EWMA model to forecast prices, as discussed in section 4.3. Just like the ANN method, the price forecast and weather forecast is used to create a revenue forecast in order to place maintenance in periods of low revenue.

## ARIMAX

The ARIMAX uses the ARIMAX model discussed in section 4.3. As in the other revenue-based opportunistic methods, the revenue is forecasted based on the weather forecast and maintenance is placed accordingly.

## PRODUCTION

The PRODUCTION method is the Production-based Opportunistic method. In this method only the weather forecast is used to forecast revenue. This is done by multiplying the power production by an energy price, that when combined with the postponement penalty results in the desired amount of maintenance done per day. According to the weather based revenue forecast the model places maintenance in the cheapest possible way.

## NAIVE

The NAIVE method is based on the same model framework. However, instead of using revenue forecast to place maintenance, the model is forced to place a certain amount of maintenance each day without access to a revenue forecast. Only when there is an exceedance of WSL or WHL for a certain day, model is forced to not place any SM. As with all the other methods CM is carried out as quickly as possible due to the high postponement penalty. The SM is spread across the whole year from January to November. The amount of quarters of SM the model is forced to carry out each day is defined as  $NAIVE_{quarters}$  with a value of 19 in the NAIVE method. The starting day of the NAIVE method is defined as  $NAIVE_{startday}$ , with a value of 1 in the NAIVE method. The sudo-code for the NAIVE method constraints are shown in algorithm 2. The *OpenTurbines* set is the turbines that are evaluated for maintenance defined in the simplification heuristic described in section 4.4.

---

**Algorithm 3** Sudo-code for the NAIVE method.

---

```
if  $NAIVE_{quarters} > 0$  then
    if  $DAY < NAIVE_{startday}$  or WHL or WSL enforced then
         $\sum_{\forall w \in W, \forall t \in T} r_{t,w}^{SM} = 0$ 
    else
         $\sum_{\forall w \in W, \forall t \in T} r_{t,w}^{SM} = \min(NAIVE_{quarters}, \sum_{\forall w \in OpenTurbines} H_w^{SM})$ 
```

---

### NAIVE summer

During the summer months access to OWF is more abundant due lower wind speeds with the lower wind speeds also resulting in a lower production. This is seen in figure 4.3 as is discussed in Cortesi et al. (2019). Therefore a second NAIVE method is created where all SM is concentrated in the summer months from April to August. Here  $NAIVE_{quarters}$  is set to 32 and  $NAIVE_{startday}$  is set to 93. The NAIVE summer method is the same as the NAIVE algorithm described in algorithm 2.

While the methods have different objectives, all methods are based on the same model framework to allow for a meaningful relative comparison. All methods have access to the same features such as:

- Physical modelling of the OWF and distances
- Fuel consumption reduction by reducing speed
- CTV tracking at each timestep
- Crew tracking at each timestep
- Enforcement of WHL and WSL

The methods will be compared to each other using several indicators. The most important indicators are given by the realized profit as presented in equation 4.11 and the lost revenue due to SM.

### Additional comparison method: Hybrid-Naive

As the performance of the different models is expected to vary significantly based on the timing and finishing time of the individual runs, it can be difficult to directly compare the performance of each model. To mitigate this effect and more directly compare methods, a modification of the NAIVE run is created where the O&M model has access to the different forecasts. Each method is forced to perform the same amount of SM each day (4.75 hours or 19 quarters), if no WHL or WSL apply. The only difference in each simulation is the quarterly placement of the 4.75 hours of SM for each day, based on the given revenue forecast. As the maintenance cannot be postponed to subsequent days the benefit of a

model with access to a revenue forecast will be smaller than with a comparison without this restriction. The technique for comparing methods explained above will be referenced as a Hybrid-Naive method.

## 4.8 CO<sub>2</sub> savings

The O&M model presented in this study includes a simplified cost of operation, where fuel cost is included as a cost variable. As the wind industry is an industry with intrinsic focus on sustainable solutions, CO<sub>2</sub> emissions are relevant to investigate. This is also the reasoning behind allowing the O&M model to save fuel by traveling slower, made possible by the time-space node approach discussed in section 4.4. To see the impact that the cost of fuel has on the decision making by the O&M model a fuel cost multiplier, or CO<sub>2</sub> tax, is introduced. The CO<sub>2</sub> tax could be an externally applied tax or an synthetic internal CO<sub>2</sub> tax applied by the OWF operator to lower CO<sub>2</sub> emissions. In this study the CO<sub>2</sub> tax is applied to the fuel cost; i.e. a 50% CO<sub>2</sub> tax corresponds to a 50% higher cost of fuel. In this study CO<sub>2</sub> emissions are assumed to be directly proportional to the fuel consumption given by the total maintenance cost, MC, divided by the cost of fuel, FC. The emissions are calculated from the expected emissions of one kilogram of fuel, and the density of fuel. Thus the emissions is given by the CO<sub>2</sub> intensity of Maritime Diesel Oil (MDO) ( $\alpha$ ) (*Marine Benchmark: 2020 global shipping CO2 emissions down 1% - Offshore Energy n.d.*) of  $3.15 \frac{\text{kgCO}_2}{\text{kgFuel}}$  and the density  $d$  of MDO of  $0.9 \frac{\text{kg}}{\text{L}}$  (Schaschke, Fletcher, and Glen 2013).

$$\text{Emissions} = \alpha \cdot d \cdot \frac{MC}{FC} \quad (4.69)$$

# 5 Results

As discussed in the methodology section, there are numerous inputs that define and influence the proposed O&M model. The inputs and the corresponding results will be presented in the following sections. Initially, the forecasts developed for each forecasting method are presented. Given the forecasts the hyper parameter tuning is presented, this will form the base of further analysis. Thereafter each schedule method will be compared in short-term cases and long-term yearly simulations. Finally a sensitivity analysis of the key parameters of the model will be done. This should provide a clear illustration of how the model works, and which parameters affect performance as well as the resultant solutions.

## 5.1 Forecasts

As the O&M model will make decisions based on the forecasted wind speed and power market price, these are a crucial part of the O&M model. In the following section the results obtained from fitting the different forecasting models will be presented. Additionally, the accuracy of the forecasting models will be compared qualitatively by comparisons of time series, as well as quantitatively evaluated using RMSE.

### Weather forecast

As mentioned in section 4.3, the weather forecasts are generated based on the true weather. Since all O&M models except the NAIVE method compared in this study relies on a weather forecast, it is important that the generated weather forecasts are realistic and have comparable accuracy to NWPs used in practice (Pathak et al. 2022; Ben-Bouallegue et al. 2022). Figure 5.1 shows the RMSE for all generated forecasts for 2022. Here the RMSE for each hour into the future is plotted. As expected it can be seen that the error increases, when forecasting further into the future.

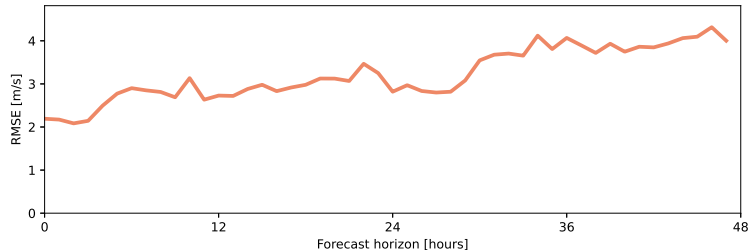


Figure 5.1: Wind speed forecast accuracy for 2022. Forecast horizon defines how far into the future the forecast is made. Accuracy is given by the RMSE of all forecasts through 2022.

In the figure 5.1 the forecasting errors lies within the bound of what is currently possible using forecasting methods such as Lam et al. (2023). It should be noted that only the wind speeds forecasted after the 12th hour are used since the model is run at 12 noon as illustrated in figure 4.4.

## Power market forecasts

The power market forecasts are compared to the actual forecasted prices in figure 5.2 for four days in 2021. Based on the days picked from 2021, it seems like the ANN and EWMA forecasting methods are able to produce the most accurate forecasts. They are able to accurately capture the overall price level, as well as most of the contours throughout the day. The relative price contours throughout the day is important for the placement of maintenance throughout the day. The absolute price level and postponement penalty determines whether maintenance will be postponed.

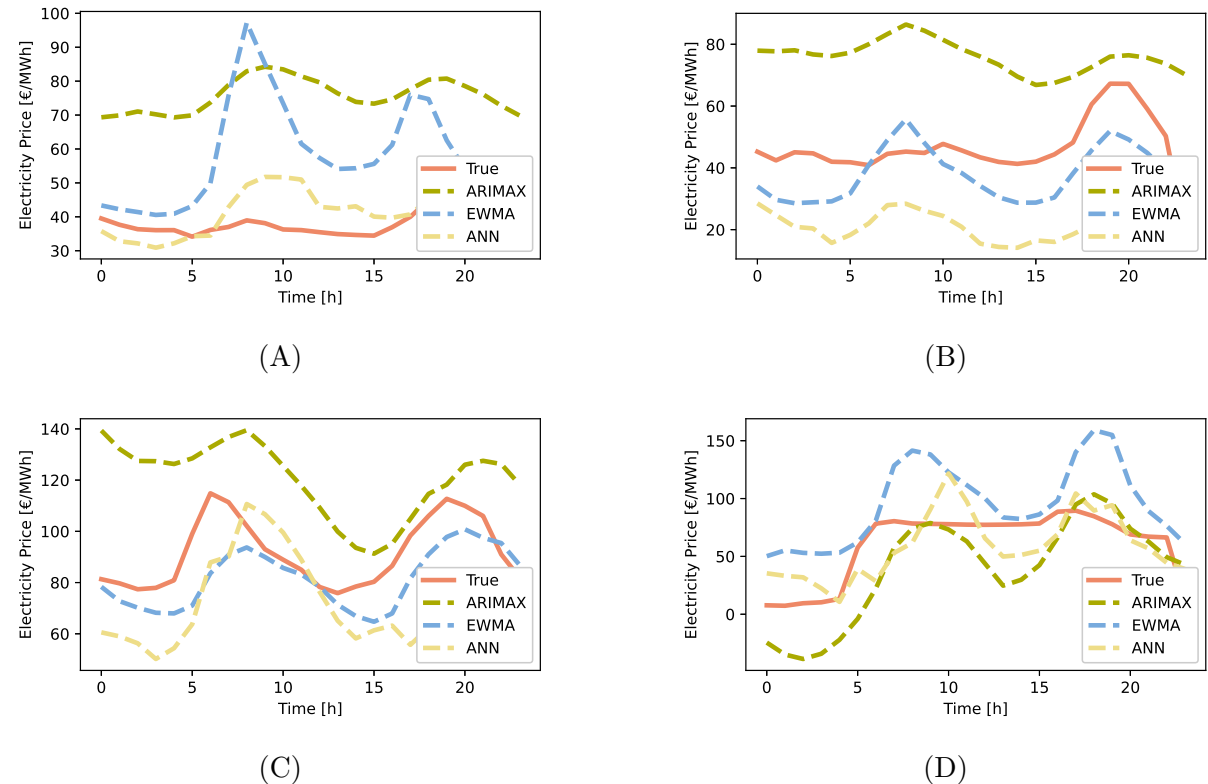


Figure 5.2: Forecasts and true power market prices for days 50 (A), 100 (B), 200 (C) and 300 (D)

## Long term accuracy of power market forecasters

In figures 5.3A and 5.3B the running RMSE can be seen for 2021 and 2022 respectively. Here the running RMSE for all three forecasting models in 2021 and 2022 are relatively similar. Note that the running RMSE is given by computing the RMSE for the future forecast for each day. In particular during the latter part of 2021 and throughout 2022

it can be seen that the forecasting error in terms of RMSE increases. In figure 5.3C and 5.3D the total RMSE and the normalized RMSE for 2021 and 2022 are plotted. Here it can be seen that the ARIMAX and EWMA have the highest accuracy in terms of RMSE in 2021, but that ARIMAX seems to be performing better than the other two forecasting methods in 2022.

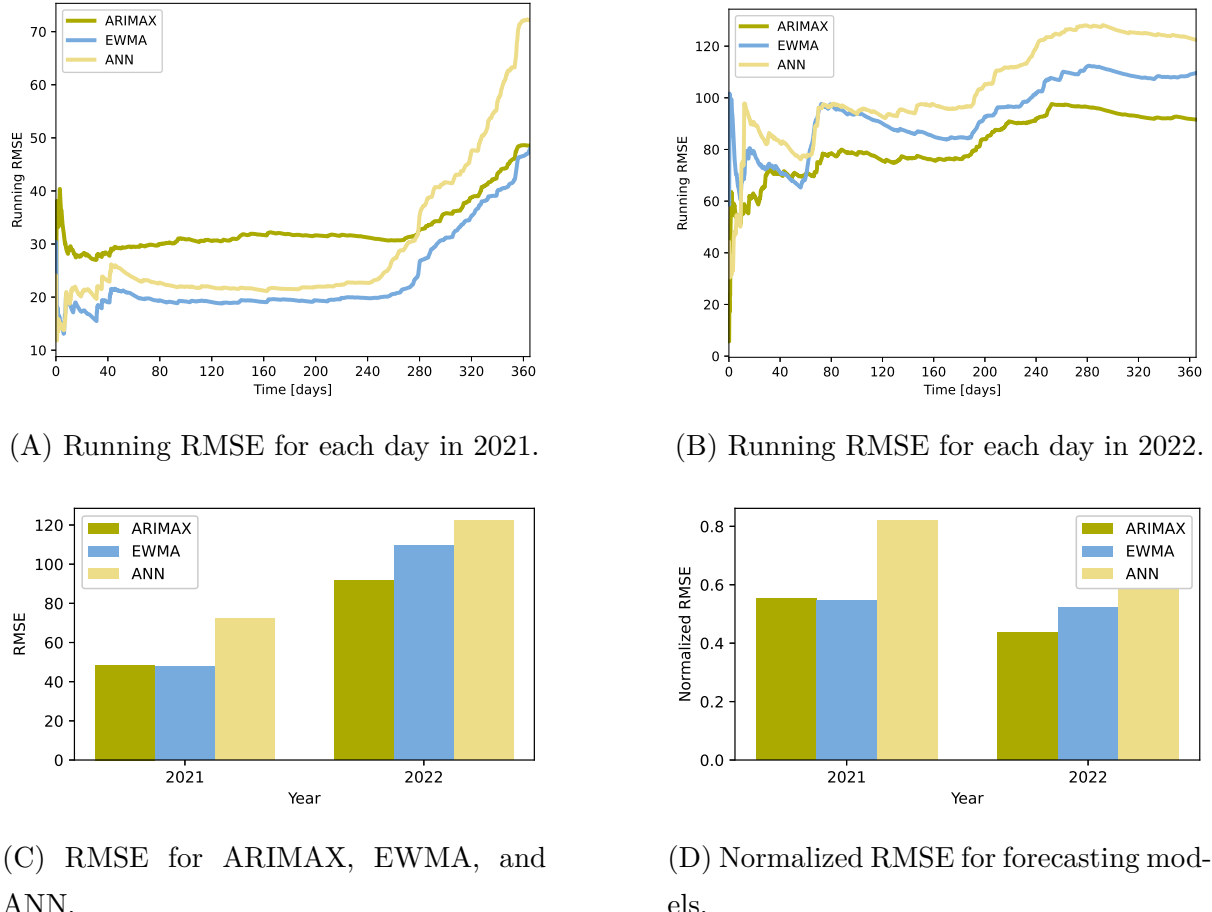


Figure 5.3: Forecasting errors for 2021 and 2022.

## 5.2 Tuning hyper parameters

When running the O&M model there are several parameters to tune. The hyper parameters include arc lookout time ( $\delta$ ) as seen in the problem formulation, planning horizon, amount of turbines included in the heuristic  $n$ , and the postponement cost. The hyper parameter tuning is carried out by running the O&M model with a sweep of the mentioned parameters for 2021.

### Planning horizon

In figure 5.4 it can be seen that there is a non-linear increase in running times with longer planning horizons. While the non-linear increase in running time is seen in both the model

definition and solving time, it is more prominent for the solving time. There is a minimal difference in the total realized profit for each model, with the one day planning horizon being less than 0.01 % worse than with longer planning horizons.

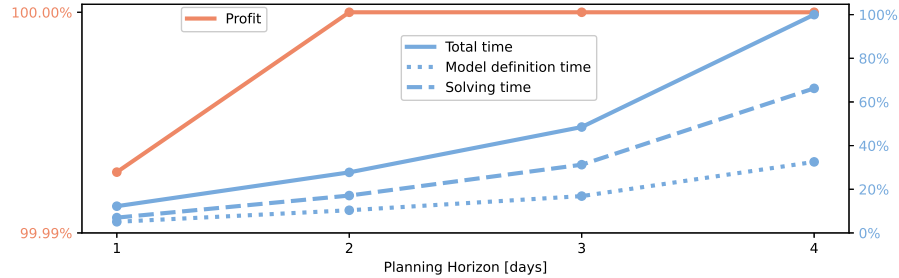


Figure 5.4: Profit and solve time as function of days planned ahead.

Test parameters: W: 36, CTV: 1, CREW: 4, Days: 31, Year: 2021

Given the minimal impact that planning horizon has on profit, a planning horizon of 1 day is used in the final model to reduce computation time.

## Arc lookout period

In figure 5.5 the computation time and realized profit can be seen as a function of the arc lookout period. The solve time rises in non-linear manner for larger arc lookout periods. For a arc lookout period of 3 the solve time is 55% that of a arc lookout period of 8 quarters. The realized profit is 0.05% higher for a lookout period of 8 compared to 3.

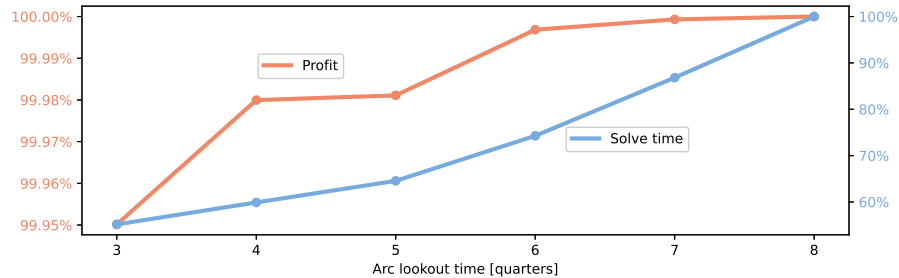


Figure 5.5: Profit and solve time as function of planning horizon.

Test parameters: W: 20, CTV: 1, CREW: 4, Days: 31, Year: 2021

To balance computational time and performance a lookout period of  $\delta = 6$  will be chosen for the final model.

## Heuristic

As discussed in section 4.4 the model becomes difficult to solve with larger amount of turbines. Therefore a heuristic to narrow the solution space is added. The heuristic narrows the amount of turbines down from  $W$  to  $W_{heu}$ , with the exact method is described in section 4.4. The method does cut off feasible solutions and potentially optimal solutions.

It is therefore important to investigate the effect of shrinking the solution space on the realised profit. In figure 5.6 the solve time relative to the slowest average solve time is shown as a function of the number of turbines included in the heuristic. To limit computational complexity, the heuristic approach is run for a model with 36 wind turbines, 1 CTV, and 4 crew over 15 days. Here it can be seen that including more turbines in the heuristic for larger values of  $n$  has diminishing returns, especially from  $n = 6$  and upwards. Since different amounts of SM is performed for each value of  $n$ , the objective value MILP model, rather than the profit, is used to compare the performance given various values for  $n$ .

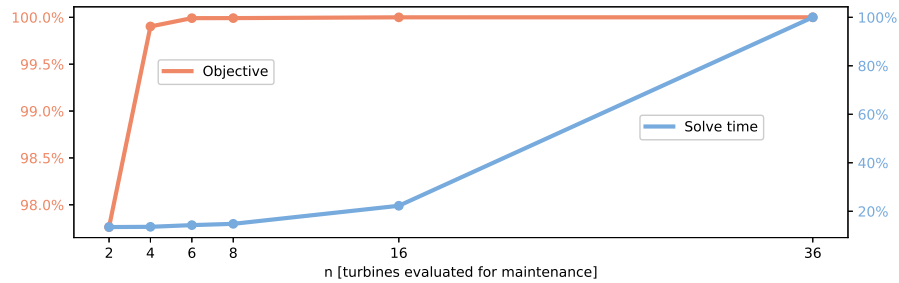


Figure 5.6: Solve time and Objective value for heuristic method.

Test parameters: W: 36, CTV: 1, CREW: 4, Days: 31, Year: 2021

To balance performance and solve time  $n = 6$  is chosen for the remainder of the study.

## Postponement cost

This section will investigate the relation of amount of SM performed and the postponement cost of SM. The postponement cost for CM is fixed and will not be investigated. The relation between postponement cost and the average maintenance done per day per crew is seen in figure 5.7. When no postponement penalty is given no SM is done, the model only performs CM. As expected the amount of SM performed increases as the postponement cost is increased. At a cost of 1000 €/hour the limit of maintenance done per day per crew is reached at 8.2 hours/day/crew. While the working day is 12 hours long, each crew cannot perform 12 hours of maintenance each day due to traveling times as well as WHL and WSL restrictions.

As mentioned in section 4.4, the postponement cost can also be defined by a quantile from the previous 6 weeks electricity prices. Performing the same analysis in figure 5.8, reveals that using the 0-100 deciles cannot reach the same amount of maintenance performed as with the fixed postponement cost. This is expected as prices of up to 1200 €/MWh are never observed. This approach is however suspected to be more adaptive to various price levels and should thereby require no tuning during a simulation run if price changes change. Thus the 80th quantile is used in further testing.

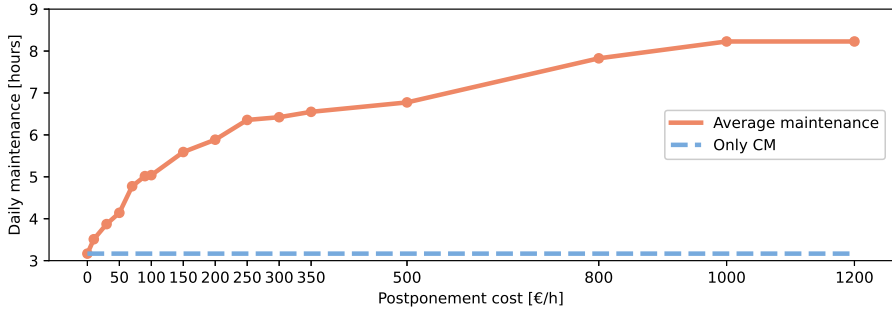


Figure 5.7: Average daily maintenance done each day per crew as function of postponement cost.

Test parameters: W: 36, CTV: 1, CREW: 4, Days: 365, Year: 2021

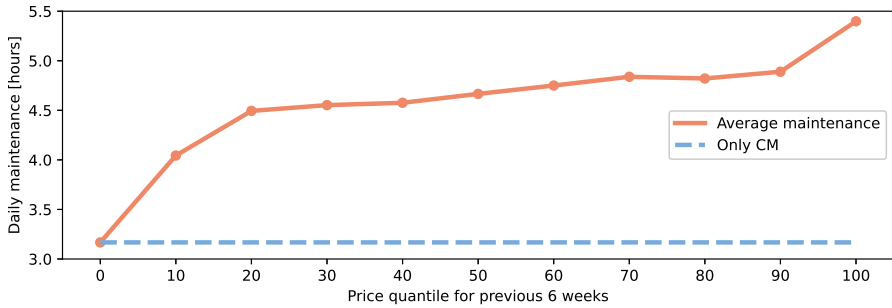


Figure 5.8: Average daily maintenance done each day per crew as function of the price quantile for last 6 weeks used as Postponement cost.

Test parameters: W: 36, CTV: 1, CREW: 4, Days: 365, Year: 2021

### 5.3 Computations

Being able to solve the model in a reasonable amount of time is essential for any practical usage of the model. In the previous section a number of hyper parameters are chosen due by balancing effect on profit and solve time. In this section the computational challenges will be investigated.

The model uses a large amount of memory and has longer solve times as the model gets larger, especially as the number of turbines and CTVs increases. As discussed in section 4.4, the amount of variables gets much larger as the wind farm scales. With a larger amount of variables the amount of time it takes to define the model also gets larger. Therefore both the model definition time, the solve time, and total computation time is shown in figure 5.9A.

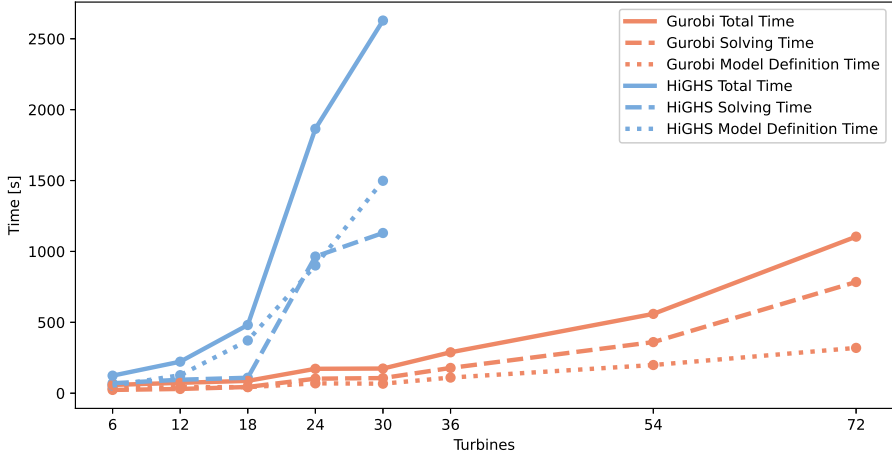
The solver used to optimize a MILP can have a large impact on the solve time. The solve time of the Gurobi solver is compared to the HiGHS solver, which is an open source solver with performance comparable to that of commercial solvers (Anstreicher et al. 2024).

Peak memory load and computation time as a function of number of turbines is shown

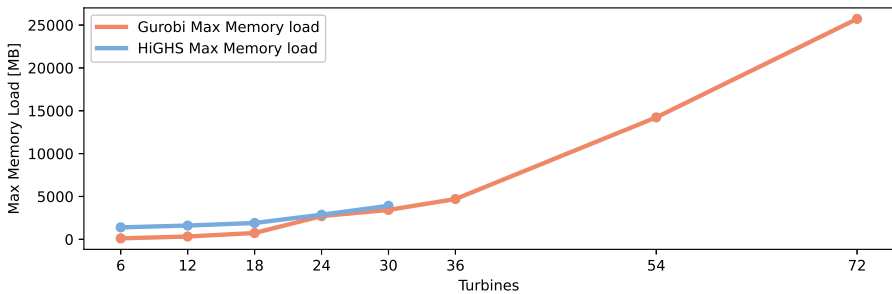
in figure 5.9 for both the Gurobi and HiGHS solver. A table format of figure 5.9 can be found in the appendix table A.4. For the Gurobi solver a non-linear increase is seen for both total solve time and peak memory as the OWF scales. The peak memory load is very comparable between the two solver, whereas the solve time for the HiGHS solver is much longer even for an OWF size of just 24 turbines.

It is evident that the Gurobi solve performs much better than the HiGHS solver on this problem, both in terms of model definition time and solve time. Therefore the Gurobi solver is used throughout this study.

Run times and memory load is highly dependent on the run parameters. The exact list of parameters used for the solve time experiment in figure 5.9, can be seen in Appendix table A.3. In the figure it can be seen that it approximately 1100 seconds to carry out a 15 day simulations. This corresponds to approximately 26800 seconds or 7.4 hours when extrapolated to a full year.



(A) Solve time as a function of number of turbines in the simulation. Both the total computation time, the time used on defining the model, and the time used on solving is shown for both the Gurobi and HiGHS solver. The HiGHS solver is only tested up to 24 turbines due to computational time.



(B) Max memory load during solve as a function of number of turbines in simulation.

Figure 5.9: Performance comparison of solve time and max memory load. For table format see: table A.4 in appendix. The HiGHS solver is only tested up to 24 turbines due to computational time.

Test parameters: W: 6-72, CTV: 1, CREW: 4, Days: 15, Year: 2021

## 5.4 Short- and long-term simulations

To understand and validate the model both short and long-term simulations are performed on 2021 and 2022. In particular the short-term results should validate the decisions made by the model on a 15-minute basis, while long run results validates the long-term performance of each model.

### Short-term CTV routing

To validate the decision making of the model, a short run is considered. The ANN-method with 4 CREWs, 1 CTV with a postponement cost defined by the 80th quantile of historic prices is used. The revenue forecast as well as the resultant decisions by model are plotted in 5.10. As expected the model uses the least time consuming arcs to reach the three turbines with CM in the fastest possible time. The difference in extra fuel cost between slower and faster arcs is on the order of 10s of €/quarter, whereas the postponement cost for CM is 1000 €/quarter as seen in eq. 4.36. On top of this is the added lost revenue as long as a turbine has remaining CM. However, once three crew have been placed for CM maintenance, the model chooses the second fastest route to turbine 13 to perform SM, and chooses the slowest route back to 15 to wait for this task to be done.

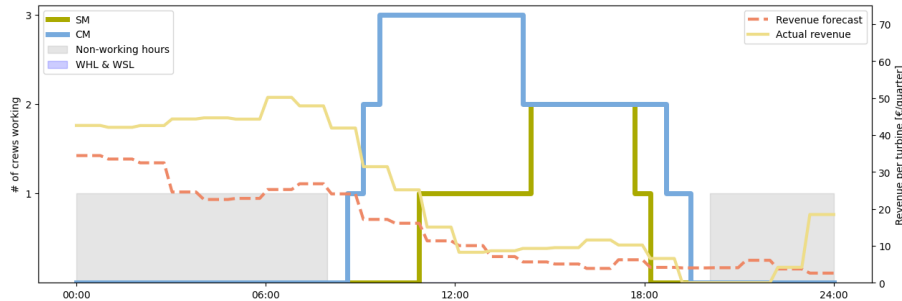


Figure 5.10: Scheduling of maintenance based on forecasted revenue using ANN for April 10th (day 99) in 2021.

Test parameters: W: 36, CTV: 1, CREW: 4, Days: 365, Year: 2021

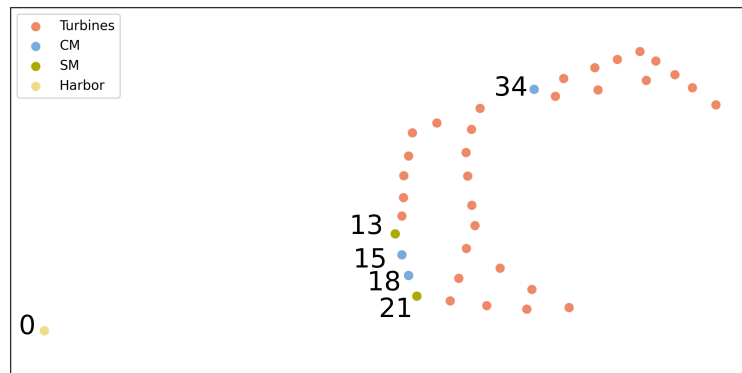


Figure 5.11: Relevant node labels for CTV routing for day 99 in 2021.

The resultant routing of the CTVs can be seen in figure 5.12. The CTV initially leaves the harbour at 8 am, this is expected as the CTV is forced to stay in the harbour overnight until this hour. The CTV then travels to wind turbine 18, where it drops off a crew to carry out CM, this process is repeated at wind turbines 15 and 34. A crew is also dropped off at wind turbine 13 to carry out SM. The CTV then travels to turbine 15 to pick up the crew and deliver them to turbine 21, where the CTV waits until SM is done for the day. Finally the CTV travels to the other turbines to pick up the remaining crew and travels back to Klintholm harbour in node 0.

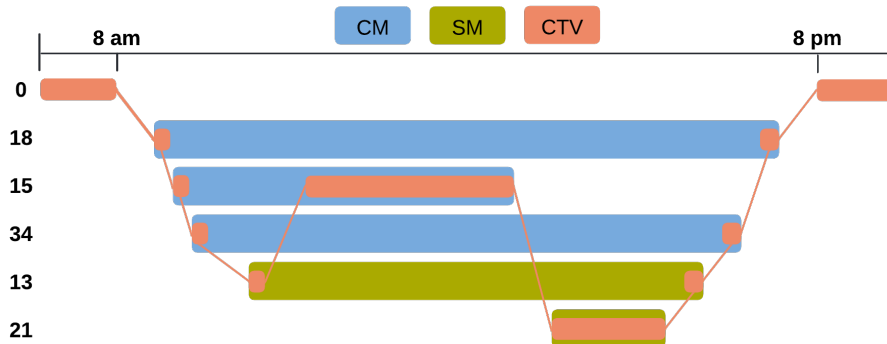


Figure 5.12: Routing of CTV for day 99 in 2021. Numbers represent each turbine with 0 representing the harbour.

## Short-term model decisions

To understand how each model decides when to place maintenance, May 14th of 2022 (day 134) from the simulation runs shown in figure 5.15 is investigated. Due to a combination of strong winds and sun May 14th 2022 had electricity prices around 0 €/MWh for most of the day until 17:00 (TV2 2022).

The PERFECT model naturally mirrors the correct price throughout the day apart from a small error during the last part of the day caused by the non-perfect weather forecast.

Given that the EWMA forecaster is an average of previous prices, the model can not forecast the extreme prices of this day, which results in a double price peak in the morning and in the evening as a result of prices on average being higher during morning and evening hours.

The ANN model creates a price forecast very similar to the EWMA model, at a too high level to perform any SM.

Of the three non-perfect price forecast models, the ARIMAX is the only one placing SM. The ARIMAX model correctly places all SM during the times of forecasted low revenue. It does however not forecast the high prices in the evening and therefore ends up having

three turbines shut down during times where each turbine could have produced around 400€ in revenue per quarter.

The PRODUCTION model predicts a constant revenue caused by forecasted strong wind throughout the day. Consequently, each turbine is expected to produce the maximum output of 8.4 MW throughout the day. The expected constant production multiplied by a fixed price of 45 €/MWh resulted in an expected constant revenue of 94.4 €/quarter/-turbine.

The NAIIVE model is forced to place 5 hours of SM each day without a revenue forecast. It places the SM at the end of the day and thereby performs SM during the high price period of the day.

The 80th price quantile for the previous 6 weeks is used as the postponement cost for all price forecasting models in figure 5.13. This results in a postponement cost for the given day of 557.24 €/hour or 139.31 €/quarter. As discussed in section 4.4 the postponement cost should be more than the lost revenue and fuel cost before the model decides to perform SM. This is especially clear with the ARIMAX model which forecasts revenues around 200 €/quarter right after dropping of the second crew to carry out CM. It has the option to perform SM directly after this but decides to wait until the forecasted prices are around 100 €/quarter. This also provides the CTV the ability to save fuel on the way to place the first SM crew. It also decides to drop off a single crew for just one hour between 16:30 to 17:30. With the very low forecasted prices during this time it can use a lot of fuel to drop off crews and still have a cost of less than the 139.31 €/quarter postponement cost.

While each methods places SM in widely different times for May 14th, the decision for each model is explainable given each methods revenue forecast, showcasing the explainability of the model.

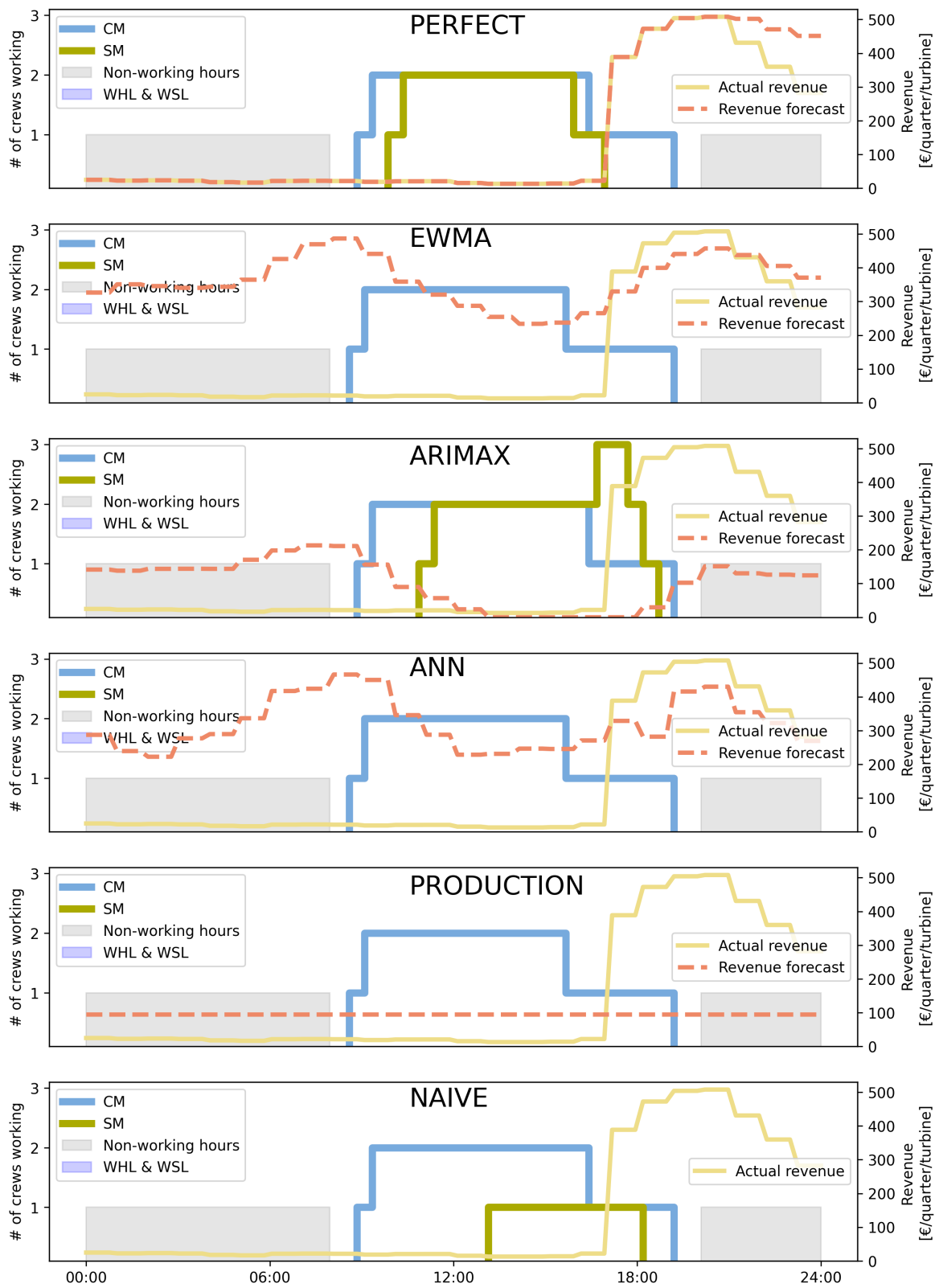


Figure 5.13: Model decision by each model on May 14th 2022. Revenue forecast given to each model is shown by the dashed line. The amount of CM and SM performed in each quarter is given by the blue and green line respectively. Grey areas represent non-working hours.

Test parameters: W: 36, CTV: 1, CREW: 4, Year: 2022

## Long-term simulations

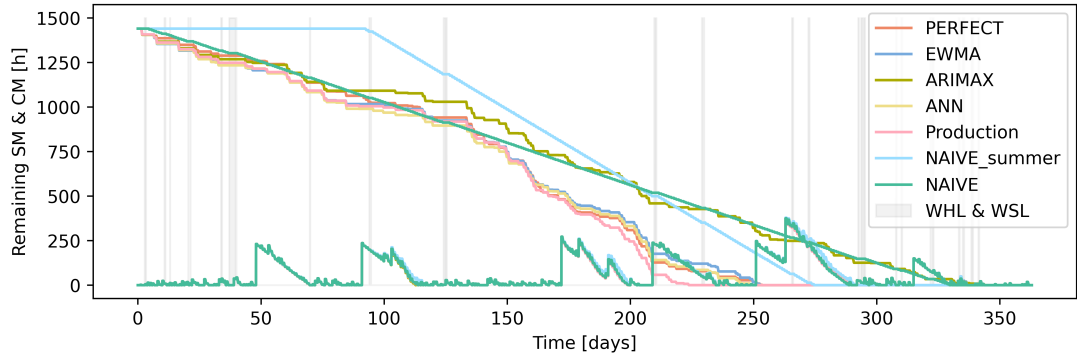
Given the short-term decisions and the iterative approach described in section 4.3 long-term simulations can be obtained. Simulations for 2021 and 2022 are performed to investigate the long-term performance on each method.

### 2021

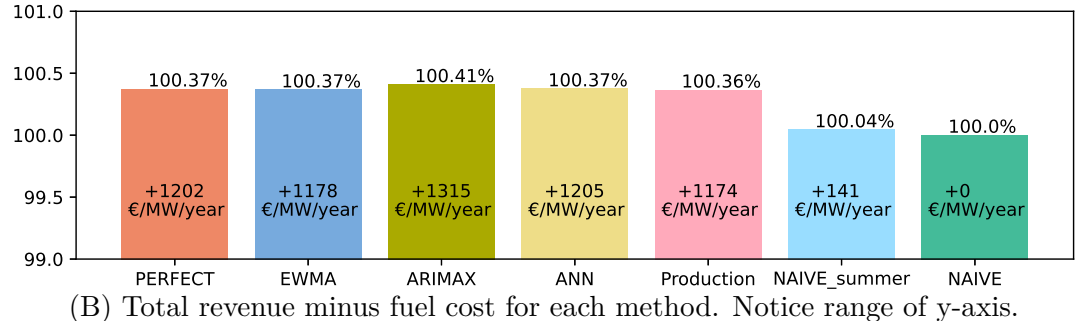
While the year 2021 has been used as a training dataset, there are still insights to be made from the performance on this year. A yearly view of the aggregated SM and CM left for each quarter is shown in figure 5.14A for each method. Here the non-increasing lines represents the amount of SM left for each turbine, and the lines near the x-axis represents the CM left. As all models carry out CM at almost the same pace, only one CM line is visible.

The total profit is shown in figure 5.14B. The lost revenue due to SM is shown in figure 5.14C. This is the revenue lost when a turbine is shut down in order to perform SM. The total cost of maintenance including lost revenue is shown in figure 5.14D. This includes turbine shutdowns during times where turbines have remaining CM, and SM is being performed and fuel cost. Here the ARIMAX model is performing better than the perfect forecast. This is most likely due to the ARIMAX simulation finishing SM significantly later than the other simulations. The reason for the later finishing time of the ARIMAX method will be discussed in section 6.3. The issue of model performance being sensitive to SM finishing time will be further discussed in section 6.3. An effort to neutralize this effect will be made in section 5.4.

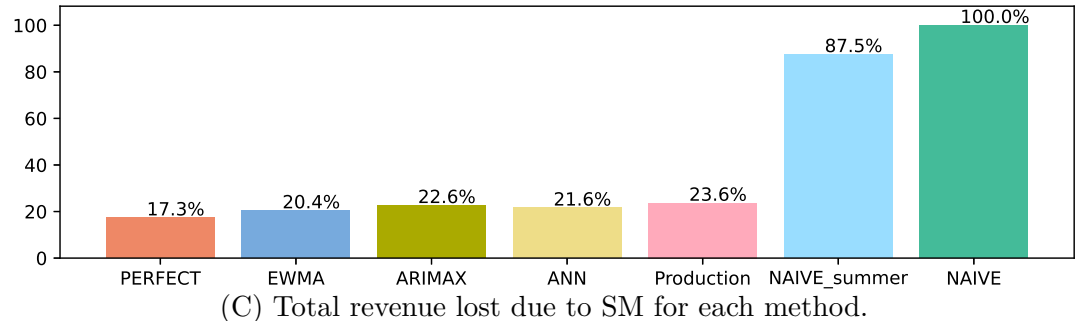
The fuel usage compared to the Naive method is shown in figure 5.14E, where all methods use less fuel than the Naive method. This is expected as the NAIVE method cannot group maintenance together on fewer days as the other methods can.



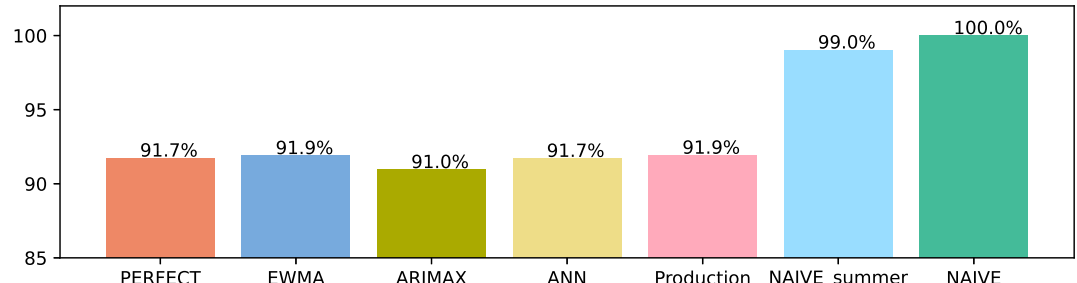
(A) SM and CM for all methods for 2021. Non-increasing lines represent remaining SM for each method and lines near x-axis represents remaining CM. Vertical lines show when WHL and WSL are enforced.



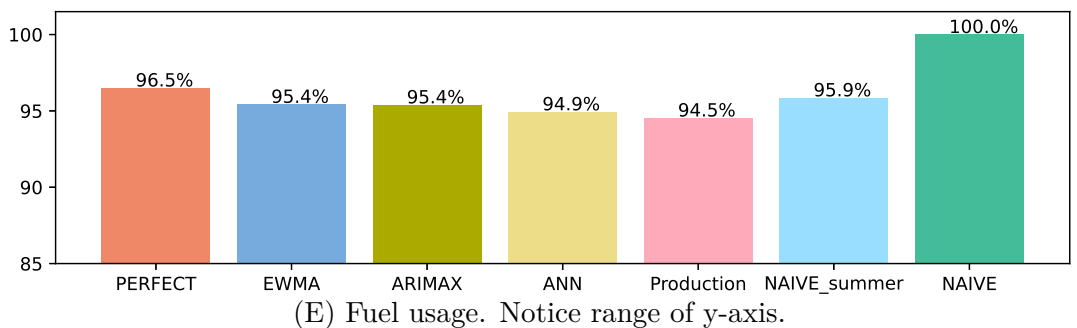
(B) Total revenue minus fuel cost for each method. Notice range of y-axis.



(C) Total revenue lost due to SM for each method.



(D) Total cost of maintenance and lost production due to maintenance, including fuel cost, and revenue lost when a turbine is shut down due to catastrophic failure or SM. Notice range of y-axis.



(E) Fuel usage. Notice range of y-axis.

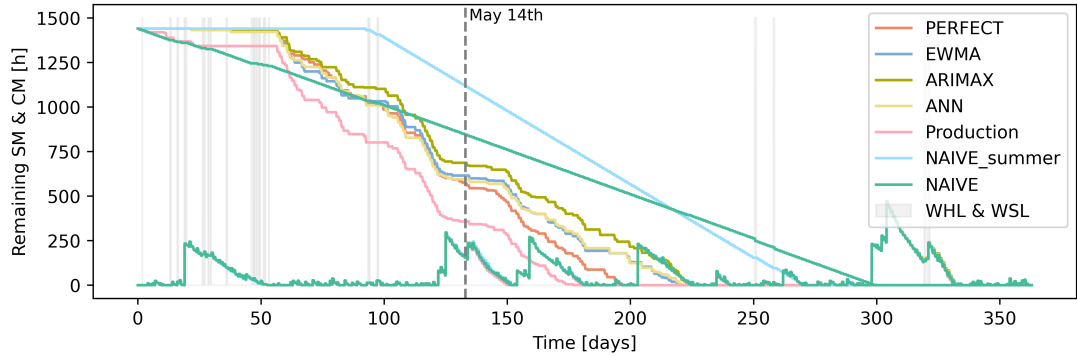
Figure 5.14: 2021 results for each method.

Test parameters: W: 36, CTV: 1, CREW: 4, Days: 365, Year: 2021.

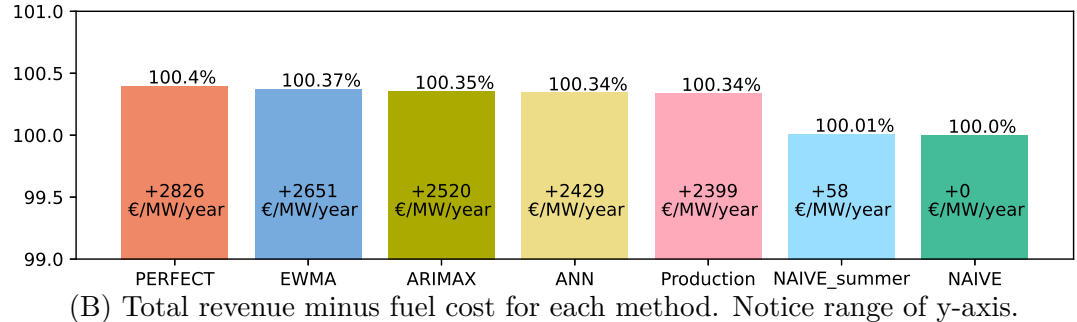
## 2022

Since the model hyper parameters are tuned on 2021, the year 2022 can be used as an unseen test dataset. Just as with the year 2021, the amount of CM and SM left for each method is shown in figure 5.15A. Here all price forecasting methods perform minimal SM before day 50. Before day 50, the WHL and WSL is regularly enforced, and a large amount of CM is present from day 20 to 50. As with the results for 2021, the finishing time is significantly different for the methods. The quantitative results in figures 5.15B, 5.15C, and 5.15D are therefore not directly comparable between each model. However the effect observed in 2021 is also seen in 2022, where the more accurate forecasts in general perform better. The revenue forecasting models have significantly different finishing times with the PRODUCTION model finishing SM around day 180 and the ARIMAX model finishing SM around day 225. The effect that finishing time has on performance will be mitigated in section 5.4.

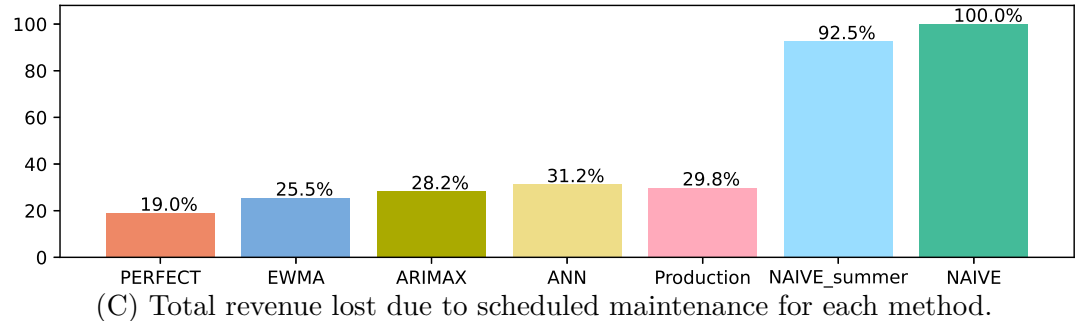
As in the case of 2021, all model use less fuel compared to the Naive method as shown in figure 5.14E.



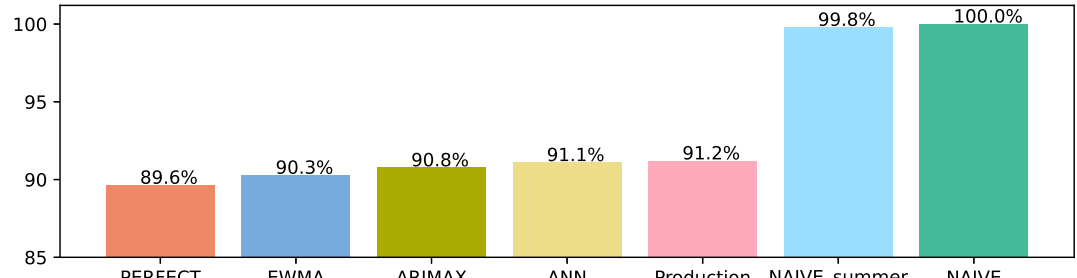
(A) SM and CM for 2022. Non-increasing lines represent remaining SM. Lines near x-axis represents remaining CM. Vertical lines represents when WHL and WSL are enforced. Vertical grey dashed line represents May 14th explored in section 5.4.



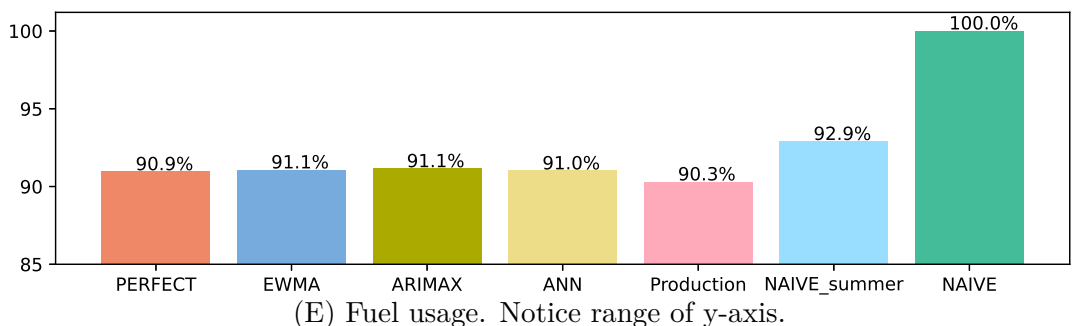
(B) Total revenue minus fuel cost for each method. Notice range of y-axis.



(C) Total revenue lost due to scheduled maintenance for each method.



(D) Total cost of maintenance and lost production due to maintenance, including fuel cost, and revenue lost when a turbine is shut down due to catastrophic failure or SM.



(E) Fuel usage. Notice range of y-axis.

Figure 5.15: 2022 results for each method.

Test parameters: W: 36, CTV: 1, CREW: 4, Days: 365, Year: 2022.

## **Long-term simulations using Hybrid-Naive approach**

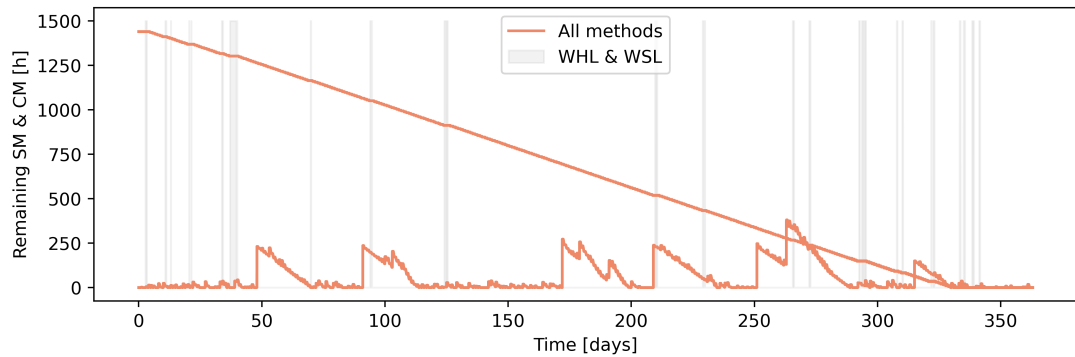
As seen in section 5.4, the performance of each method highly depends on the finishing time of the method, i.e. when the SM is done for the year. Therefore the Hybrid-Naive method is used to compare each method. The corresponding figures to the methods described can be seen on the following two pages.

### **Hybrid-Naive - 2021**

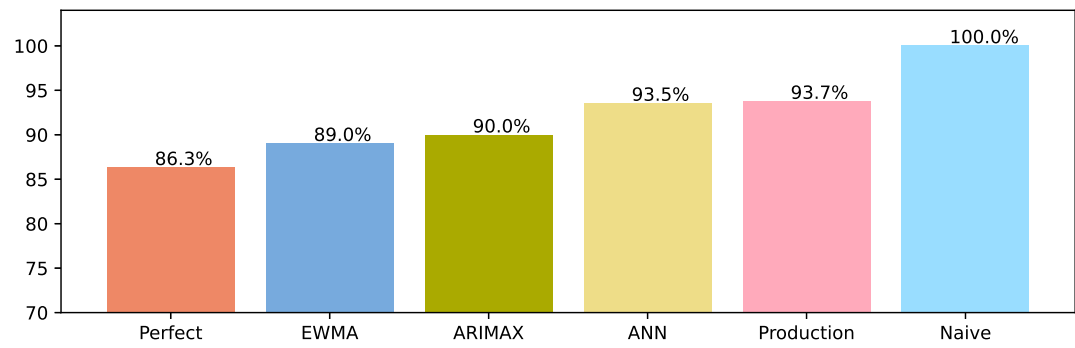
As seen in figure 5.16B the performance difference in regards to lost revenue due to SM is significant both when comparing the NAIVE run, to the production-based run, and the price forecast methods. Looking at the fuel consumption in each method in figure 5.16C, it is clear that the NAIVE method uses the least fuel, with 92.8% fuel used compared to the ANN method. This is to be expected since the nature of the NAIVE method, does not give it the incentive to quickly do maintenance to avoid a potential high-price or high-production scenario later in the day.

### **Hybrid-Naive - 2022**

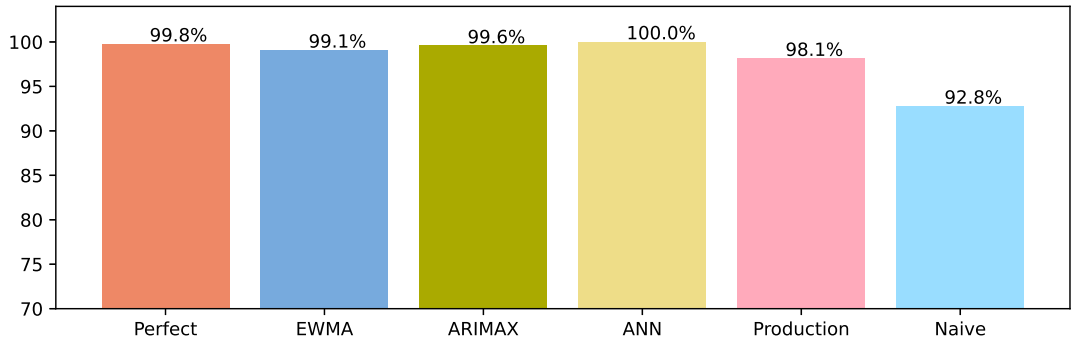
The Hybrid-Naive method has also been tested for the year 2022 shown in figure 5.17A. Here a similar trend as for 2021 is seen for lost revenue due to SM and fuel consumption. Here all price forecasting methods perform better than both the PRODUCTION and NAIVE method. For both 2021 and 2022 the NAIVE method has a fuel consumption that is between 91-93% relative to the price forecast methods. However, a significantly lower lost revenue compared to NAIVE is seen in 2022 compared to 2021. The PERFECT and EWMA model loses 75.6% & 80.7% revenue due to SM as opposed to 86.3% & 89.0% for 2021 compared to the NAIVE method. This is in line with the general trend of larger differences in models for 2022 compared to 2021, most likely due to a higher price difference. This will be further discussed in section 6.3.



(A) Comparison run using hybrid-naive framework for 2021.



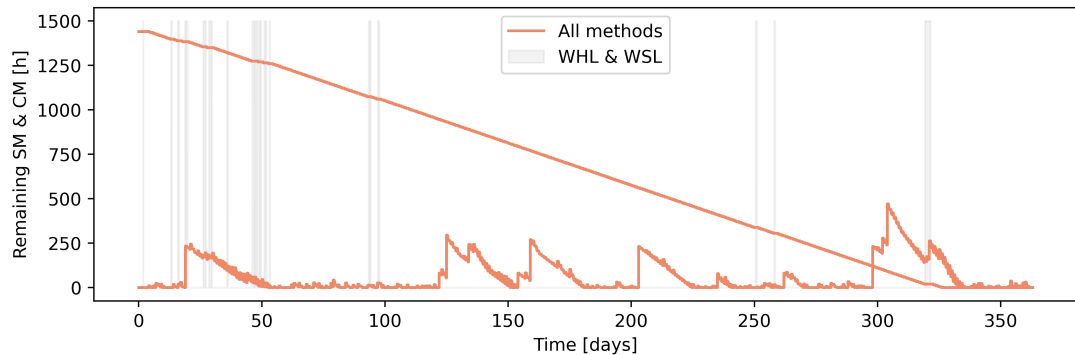
(B) Lost revenue due to SM for each method using the hybrid-naive framework. Notice range of y-axis.



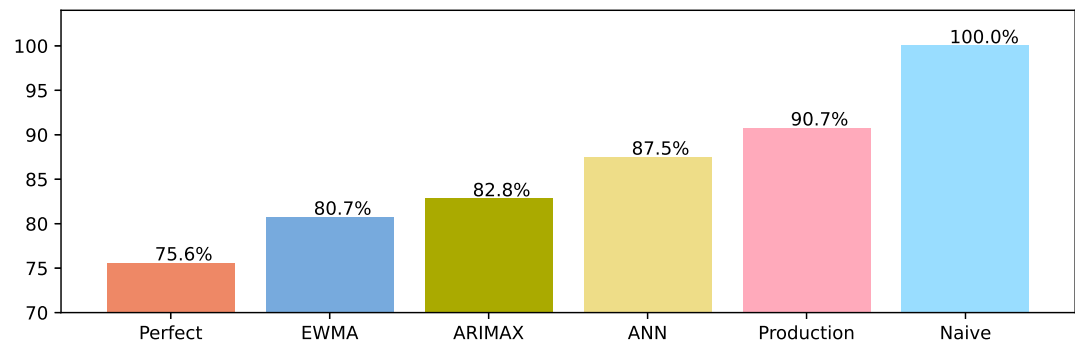
(C) Fuel consumption for each method using the hybrid-naive framework. Notice range of y-axis.

Figure 5.16: Comparison of methods using hybrid-naive framework for 2021.

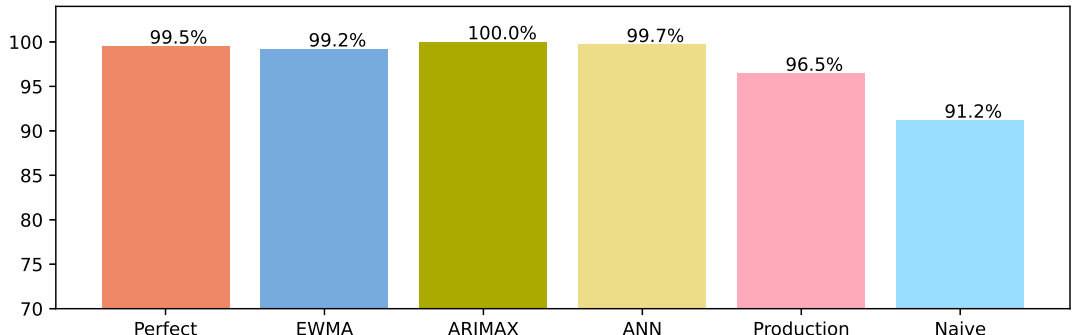
Test parameters: W: 36, CTV: 1, CREW: 4, Days: 365, Year: 2021.



(A) Comparison run using hybrid-naive framework for 2022.



(B) Lost revenue due to SM for each method using the hybrid-naive framework. Notice range of y-axis.



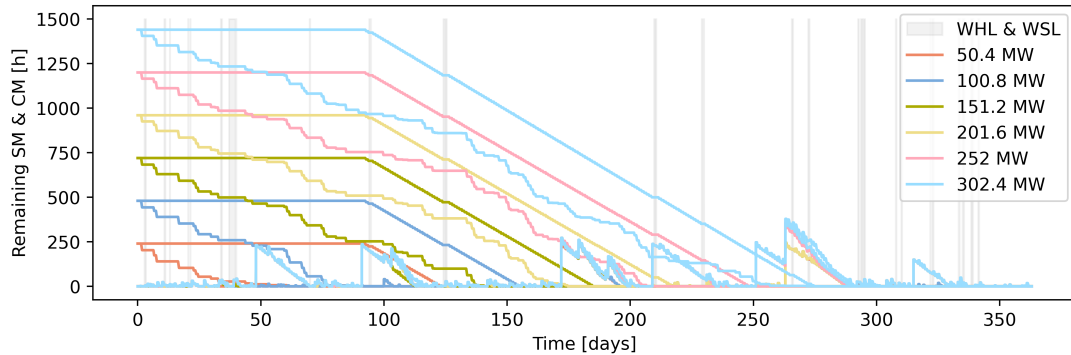
(C) Fuel consumption for each method using the hybrid-naive framework. Notice range of y-axis.

Figure 5.17: Comparison of methods using hybrid-naive framework for 2022.

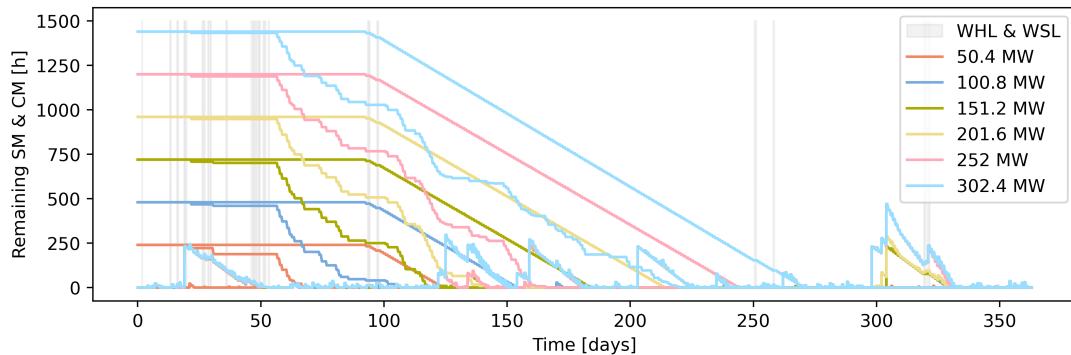
Test parameters: W: 36, CTV: 1, CREW: 4, Days: 365, year = 2022.

## 5.5 Profit increase per MW installed capacity

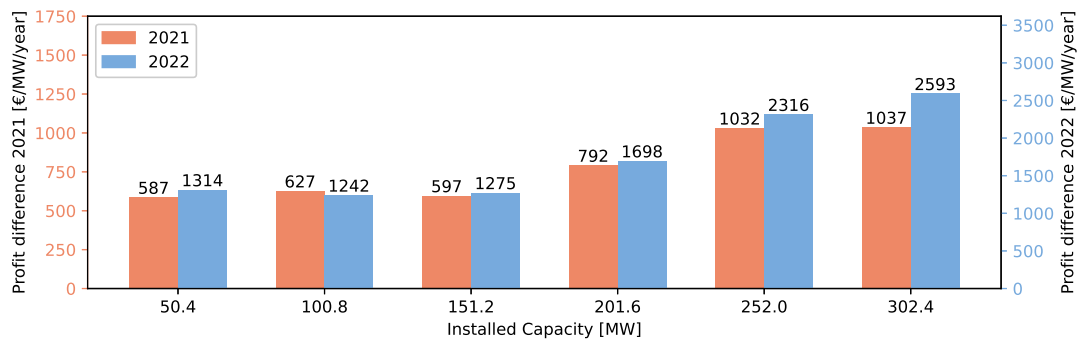
Applying a forecasting method to the scheduling of maintenance has an added benefit as seen in the previous sections. However, the additional profit per MW installed capacity might vary as the OWF size scales. Therefore the added profit by applying the EWMA method over the NAIIVE method, has been investigated for both 2021 and 2022 in figure 5.18. As in section 5.4, the relative performance of the price forecasting methods compared to the NAIIVE is significantly higher in 2022 compared to 2021, but follows to follow the same upwards trend.



(A) Model run for each OWF size in 2021.



(B) Model run for each OWF size in 2022.



(C) Added profit by applying EWMA method over NAIIVE summer simulation method for 2021 & 2022.

Figure 5.18: Comparison of OWF size and added profit for 2021 and 2022.

Test parameters: W: 6-36, CTV: 1, CREW: 4, Days: 365, Year: 2021 & 2022

## 5.6 Sensitivity Analysis

It is essential to understand the robustness of the proposed model and how sensitive it is to input changes. Given the hyper parameters determined in section 5.2 the O&M model is run with a sweep of variations to key model parameters.

### CO<sub>2</sub> Tax

To investigate the effect of changing fuel cost simulations are made with changing levels of a CO<sub>2</sub> tax applied. As described in section 4.8 the CO<sub>2</sub> tax applied in figure 5.19 is a multiplier added to the fuel price, i.e. a CO<sub>2</sub> tax of 0% corresponds to the original fuel price of 0.25€/liter and a CO<sub>2</sub> tax of 100% corresponds to a fuel price of 0.5€/liter.

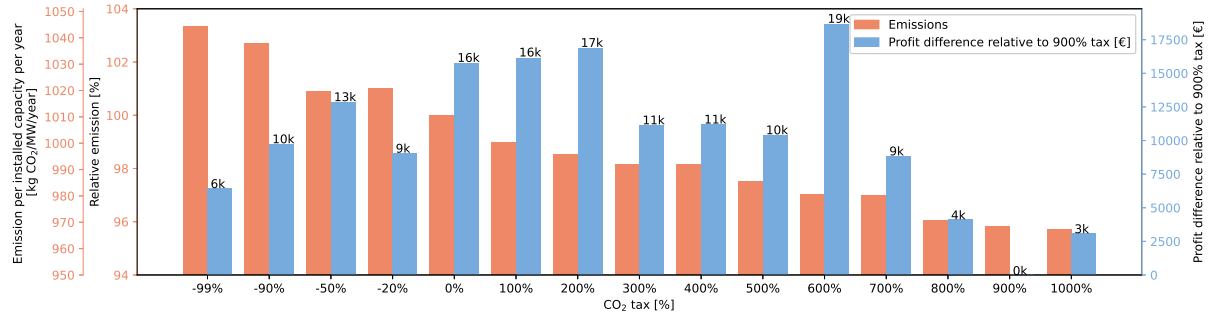


Figure 5.19: CO<sub>2</sub> emission as a function of CO<sub>2</sub> tax applied.

Test parameters: W: 36, CTV: 1, CREW: 4, Days: 365, Year: 2021

The starting point of 0% CO<sub>2</sub> tax yields an emission of approximately 1010  $\frac{\text{kg}}{\text{MW}\cdot\text{year}}$ . As seen in figure 5.19, a general trend of lower CO<sub>2</sub> emissions are seen as the CO<sub>2</sub> tax is increased. Moreover, it is seen that using a CO<sub>2</sub> tax does not necessarily reduce the overall profit as seen in the example of going from 0% to 600%, where the profit is higher with the CO<sub>2</sub> tax applied.

### Crew sensitivity

The number of crews available to the model will change how quickly maintenance can be done. Having many crews will allow the model to quickly finish CM and SM tasks, potentially leading to a saving in lost revenue. Having additional crews will come with a larger expenditure in crew salary. The crew salary expenditure is not incorporated in the model.

In figure 5.20 the 6 runs with various number of crews can be seen. In the figure the different runs finish at different times, where the runs with 1, 2, and 3 crews do not manage to finish the remaining maintenance within the year. Resultantly in table 5.1 it can be seen that the three understaffed runs lose a significant share of the potential revenue due to the inability to do CM in a timely manner. For the simulation of only 1

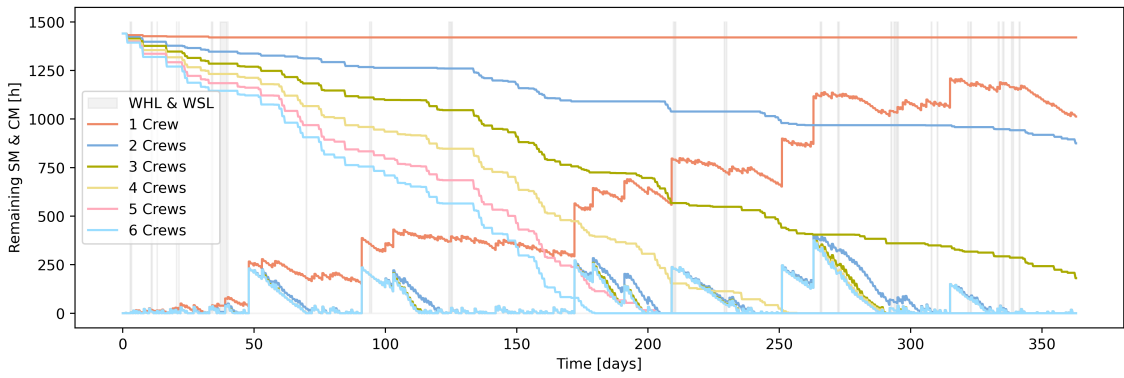


Figure 5.20: Sensitivity analysis of number of CREW with 1 CTV available.

Test parameters: W: 36, CTV: 1, CREW: 1-6, Days: 365, Year: 2021

Table 5.1: Financial difference from case with 6 Crew. Note that 1, 2, and 3 crew are not done within the year and are therefore not comparable.

Test parameters: W: 36, CTV: 1, CREW: 1-6, Days: 365, year: 2021

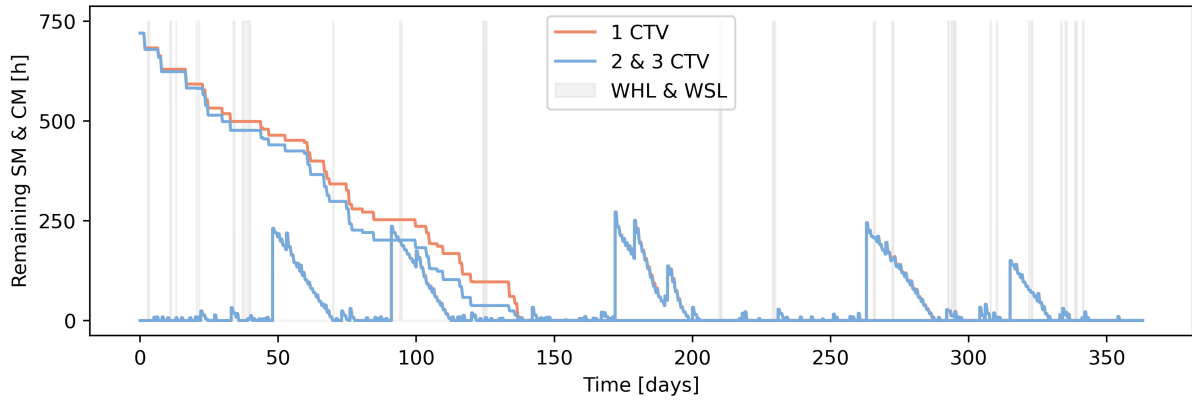
CREW	1	2	3	4	5	6
Done within the year				✓	✓	✓
Lost revenue due to CM diff. [k€]	30,168	1,056	85	20	1	0
Lost revenue due to SM diff. [k€]	-68	-19	27	6	-2	0
Fuel Cost diff. [k€]	-15	2	2	1	1	0
<b>Profit diff. [k€]</b>	<b>-30,084</b>	<b>-1,038</b>	<b>-115</b>	<b>-27</b>	<b>-0</b>	<b>0</b>

crew the model correctly prioritises CM over SM and therefore ends up performing near zero quarters of SM. Moreover, it is clear that having only 1 crew is not enough to perform all CM as the remaining CM keeps increasing throughout the year. In the table it can be seen that once the number of available crews surpasses the threshold level such that all maintenance is done, there is minimal gain from adding additional crews.

## CTV sensitivity

While the number of crews can have a major impact on the maximum number of task done at once, the number of CTVs can have an impact on how fast the crews are dropped off. This can however result in additional fuel consumption and thus additional expenditure in fuel. Moreover, there will be an additional cost of owning or leasing extra CTVs, which is not incorporated into the model.

As seen in figure 5.21A, the maintenance is finished in a quicker time frame with 2 and 3 CTVs compared to only 1 CTV. However, adding the third CTV over the second seems to make a minimal difference as to when the SM is done. In figure 5.21A only the runs with 1 and 2 CTVs are plotted, as the run with 3 CTVs is visually identical to the run



(A) Sensitivity run with 1, 2 and 3 CTVs. Simulation with 2 and 3 CTVs are visually identical.

	1 CTV	2 CTV	3 CTV
Total cost of maintenance and lost revenue	100.0%	99.4%	99.4%
Total fuel usage	73.1%	95.1%	100.0%
Total solve time [s]	1749	15622	16139

(B) Comparison of lost revenue due to SM, total fuel cost, and solve time for runs with 1, 2, and 3 CTVs.

Figure 5.21: Comparison of runs with different numbers of CTVs.

Test parameters: W: 18, CTV: 1-3, CREW: 4, Days: 365, Year: 2021

with 2 CTVs. Looking at the lost revenue due to SM and fuel usage in table 5.21B there is a slight difference between the runs with 2 and 3 CTVs. As with the fuel usage there is a large difference between 1 and 2 CTVs of approximately 20%, and a smaller difference between 2 and 3 CTVs of approximately 5%. The solve time for multiple CTVs is significantly higher than that of 1 CTV. This can prove to be a problem, if the model is applied to an OWF where multiple CTVs are necessary. This issue is further discussed in section 6.4.

# 6 Discussion

In the following sections the results are examined to understand their implications. This discussion will outline how the proposed O&M strategy impacts current methodologies and highlights the novelty of the proposed model. The robustness of the developed model will be evaluated, and key limitations and assumptions will be analyzed. Finally, future directions for improving the model will be presented.

## 6.1 OR model architecture

The architecture of the OR model employed in this study allows for a development of a detailed maintenance plan on a quarterly basis while creating long-term simulations. This is made possible by the use of a virtual model of the physical OWF with the implementation of a time space node approach.

As mentioned in section 4.4 the time-space node approach is employed to allow for a detailed CTV routing in the planned schedule. One of the main challenges is the different travel times between nodes, while still keeping track of CTVs throughout the day. This is successfully solved by employing the time-space node approach as seen in Zhang et al. (2017). This enables several key benefits, such as optimizing fuel consumption as well as generally keeping track of the locations of the CTVs as well as crews.

To enable long-term simulations the OR model is run in an iterative fashion, where a daily optimization of the future plan is created. This allows for both a detailed CTV and crew routing plan for each specific day, and aggregate results to evaluate the long-term performance of an O&M strategy.

## 6.2 Hyper parameter tuning

Performing a hyper parameter tuning allows for a correct choice of parameters where the performance and computation time is balanced.

### Planning horizon

The O&M model in this project has the ability to plan and place maintenance multiple days ahead. It is therefore anticipated that allowing for more days planned ahead, will result in a better performance. However as seen in figure 5.4, there is no significant difference in profit with a longer planning horizon. Therefore a planning horizon of 1 day is chosen, as this poses a minimal comprise in regards to solution quality and a large improvement in regards to solve time. There are several factors that could explain the minimal difference in performance between the runs. It is most likely mainly due to the

OR model architecture where the decision made in day  $d$  does not significantly affect the solution in  $d + 1$ , especially with large amounts of SM remaining. This is driven by the fact that the CTVs and the crews must return to harbour during the night, and thus the plans of  $d$  and  $d + 1$  are somewhat independent of each other.

To make greater use of the longer planning horizon, one could force the OR model to do a fixed amount of SM over the planning horizon, thus also removing the need for the fictitious postponement penalty. However, this would force the model to place maintenance in high-price periods if longer periods of high prices are present.

## Arc lookout period

The primary challenge of implementing the time-space node approach is the exponential growth of arcs in the network as the number of time-space nodes increases. This is outlined in figure 4.11, where the number of arcs increases exponentially with the planning horizon. To reduce the number of arcs in the network, an arc lookout period is introduced, which limits the amount of time steps into the future that arcs are generated. Arcs are generated  $\delta$  steps into the future. With this implementation the number of arcs scales linearly with the planning horizon. Thus a large improvement in computational speed is seen in figure 5.5 without any significant reduction in the quality of the solution. Because of this the chosen arc lookout period of 6 reduces the computation time by approximately 25% compared to an arc lookout period of 8, while being less than 0.005% worse in regards to profit.

## Heuristic approach

The heuristic is implemented by constraining the model with the heuristic constraints to only consider doing maintenance on  $n$  turbines, and relying on the presolve functionality to remove this part of the solution space. As seen in figure 5.6 the matheuristic approach of defining a smaller solution space for the model dramatically reduces the computational complexity of the model and still yielding a near optimal solution. The OR model still scales non-linearly with the model size, but at a much slower rate. Thereby the chosen number of turbines to be included in the matheuristic,  $n$ , of 6 turbines poses a near zero decrease in the objective function.

The size of the OWF and number of crews are most likely very important in regards to the chosen value of  $n$ 's effect on the objective function. If applied to a large OWF with more crews than  $n$ , the effect on the objective would most likely be significant. It is therefore essential to investigate the effect of  $n$  for a larger number of crews before implementing on larger OWF sizes.

Moreover, when using multiple CTVs it might be beneficial to modify the heuristic to

create a cluster of turbines with maintenance per CTV. If using two CTVs the two turbines with most CM could be used to create two clusters instead of a single cluster as implemented in this study.

## Postponement cost

Due to the iterative approach of the OR model using a finite planning horizon unfinished maintenance needs to be punished by a postponement cost. As seen in section 5.2, the average maintenance done per day increases with an increase in postponement cost. Thus this modelling parameter has a large impact of the decision making of the model.

In figure 2021 there are two effects working in opposite directions, the first one being the fact that a lower postponement cost allows the model to be more selective and thus should provide a higher overall profit. However as seen in 2021 there was a significant increase in the overall price level of electricity approximately 8 months into 2021. This has a significant impact on the resultant profit of simulations for this year seen in figure 5.14B. Simulations that finish the SM task faster, does not have to shut down turbines in the higher price environment in the latter part of 2021. This makes the comparison between postponement costs difficult to do on the basis of 2021, but it can be concluded that a higher postponement cost overall results in the maintenance being done in a shorter time frame as expected.

While a fixed postponement cost allows for a clear threshold of when to perform SM it is vulnerable to long-term price changes. The alternative of a fixed postponement cost, using quantiles of historic prices, performs as expected. However, as seen in the long-term results it is still difficult to tune the finishing time of SM using method. The quantile approach is selected due to its adaptive nature to price changes and ease of implementation. However, creating a method that can reliably finish SM in a desired amount of time would be a great addition to the work presented in this study.

## Computational complexity & solve times

As mentioned in section 6.1 the time-space node approach is able to track CTVs throughout the OWF. This however comes with computational complexity. In this study an approach of limiting the amount of variables in the model is proposed, which consists of both limiting the amount of arcs in the network given by an arc lookout period  $\delta$  as well as employing a matheuristic that reduces the solution space. By introducing the matheuristic, planning horizon, and arc lookout period the model complexity is significantly reduced without a significant compromise to the solution quality.

Additionally, deploying the iterative architecture of only redefining day-specific constraints, as compared to redefining a whole new model for each day, allows for a tenfold computa-

tional improvement when running long-term simulations.

However, the model still requires additional work in regards to its computational performance, which will be further discussed in the discussion section on model limitations.

## 6.3 O&M Model Performance

The overall research question of this study is whether or not optimizing for revenue-based availability is better than production-based availability and the more naive methods closer to what is implemented in practice. It is therefore essential to see how each model performs both on a single day basis and on an long-term aggregated level.

### Short-term performance

In section 5.4 a case study for April 10th 2021 is done using the ANN model. This case study shows that the model is able to correctly prioritize when to use extra fuel in order to quickly perform maintenance, and when to conserve fuel in times of no rush, as when waiting for crews to finish maintenance. Additionally, the routing of the CTV seems to be near optimal when taking into consideration that CM is prioritized over SM.

The short-term decision making presented in figure 5.13 showcases how the O&M is able to effectively place maintenance in periods of expected low revenue based on the provided revenue forecast. It is apparent that the forecasts have to be accurate to provide a solid foundation for optimally placing SM. In the presented day it is a mistake not to place SM during the near zero price period. While the EWMA does miss out on an revenue-based opportunity due to its inaccurate forecast for May 14th, it does perform almost as well as the PERFECT model in the long-term simulations.

### Long-term performance

To answer the research question of whether maintenance can be placed according to a revenue-based approach and provide an improvement to the existing production-based approaches a long-term quantitative method performance comparison is made. This is presented in figure 5.14 and 5.15 for 2021 and 2022 respectively. For both years the price- and production-based models outperform NAIIVE methods. This holds for both the total profit, lost revenue due to SM, total cost of maintenance, and the amount of fuel used. Moreover, for both 2021 and 2022 the PERFECT and two price forecasting methods with the highest price forecast accuracy, EWMA and ARIMAX, outperform the PRODUCTION method in terms of lost revenue due to SM and total profit. This indicates that there is an added benefit of using a revenue-based availability O&M strategy over a production-based availability strategy.

However, the results are sensitive to the finishing time of SM as seen by the ARIMAX

model outperforming the PERFECT model for 2021 due to its later finishing time. This difference in finishing time is driven mainly by the postponement penalty approach and the price level forecast by each method. When the forecasts are relatively higher than the other methods, for instance for ARIMAX in 2021, the method expects higher revenues on average and therefore has fewer low revenue opportunities. This results in the later finishing time for SM. This is supported by the finishing times observed in figure 5.14A and the corresponding mean forecasted price in table 6.1.

Table 6.1: Mean forecasted prices for each model in 2021 and 2022.

Model	PERFECT	EWMA	ARIMAX	ANN
Mean forecasted prices [€] 2021	89	85	99	58
Mean forecasted prices [€] 2022	211	212	218	193

To determine whether the forecasting models can on average improve the O&M decision making process, the hybrid-NAIVE approach is used. This removes the uncertainty in finishing time driven by the postponement penalty approach and allows for a direct comparison between models and their corresponding performance. In figure 5.17B it can be seen, that when all methods are forced to carry out the same amount of SM every day, the methods employing power market price forecasts are on average able to better place SM in low revenue periods resulting in higher long-term revenue. Thus the results establish an added benefit of optimizing revenue-based availability compared to production-based availability.

The overall price level when simulating the use of the O&M model has an significant impact on the potential additional revenue. When considering the additional profit (€/MW/year) compared to the NAIVE method in figure 5.14B and 5.15B, it is evident that the methods perform relatively better in 2022. The additional profit (€/MW/year) for 2022 is 125% higher compared to 2021 for the EWMA model. This can be explained by higher prices seen in 2022 compared to 2021 as shown in table 6.2. Here the prices were on average 129% percent higher in 2022 compared to 2021, which is very close to the 125% performance gain seen in 2022 compared to 2021.

Table 6.2: Mean prices and standard deviation of prices in 2021 and 2022.

	2021	2022
Mean price [€]	89	204
Std. of prices ( $\sigma$ )	69	149

Given the improved performance in high price level and volatile environments, the proposed O&M model is more relevant than ever due to the increase in volatility and prices

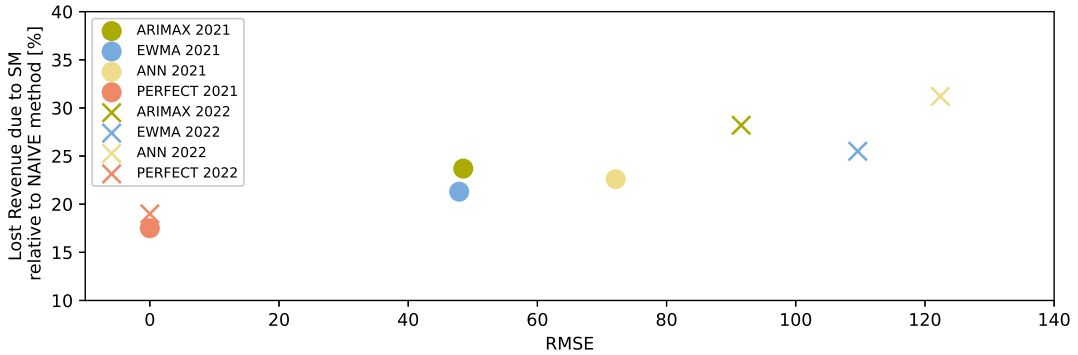


Figure 6.1: Lost revenue as a function of forecasting accuracy

observed after the energy crisis in the second half of 2021.

Given the demonstrated improvement in revenue using the proposed O&M model, it is important to ensure that the results can be generalized to other OWF sizes. By simulating the O&M activities at different OWF sizes for both the EWMA and NAIVE methods, the added benefit of implementing a revenue-based strategy over a Naive strategy can be seen as a function of the installed capacity. In order to limit the computational time long-term results are only generated up to 36 turbines equivalent to 302.4MW of installed capacity. The results in figure 5.18C indicate that there is an additional benefit of revenue-based O&M compared to a NAIVE method when considering larger OWFs. The reason behind improved performance with larger OWFs is difficult to determine due to the complex nature of O&M activities and the complexity of the developed model. Most likely the added benefit of larger OWFs arises due to the relatively more steady availability of CM opportunities. However, to fully conclude on the reason behind the added benefit for larger OWF sizes further analysis is required. Moreover, running results on the full size of Kriegers Flak of 72 turbines could give greater insights into how the added profit scales with size.

## Performance and forecasting accuracy

As observed by the long-term simulations there is a performance difference between the methods using forecasted revenue compared to the PERFECT method. This is especially clear for the Hybrid-NAIVE simulation in figures 5.16B and 5.17B. For the simulations using the postponement penalty, in figures 5.14B and 5.15B, the difference is less pronounced. For the hybrid-naive comparison the added benefit of the PERFECT method over the EWMA method comes from the PERFECT model placing SM at different hours. Whereas considering the general long-term simulations the decision becomes a question of whether or not to place SM on a specific day. The general daily price level should be easier to predict than the hourly price. This is suspected to be the reason for the more pronounced difference in performance between the PERFECT and EWMA method for the hybrid-naive approach.

Figure 6.1 illustrates that lower forecasting error, measured by RMSE, generally results in lower lost revenue due to SM. However, this is a general trend as shown by ARIMAX and EWMA for 2022 where a lower RMSE is not always better when applied in an O&M strategy.

## 6.4 Sensitivity analysis

Based on the results from the sensitivity analysis in the results section, several insights can be obtained about the model as well as some of the input parameters.

### Emission reduction

In the CO<sub>2</sub> tax sensitivity analysis, the emission from the CTVs is investigated when a CO<sub>2</sub> tax is applied. Here an approximation is made where the CO<sub>2</sub> emission is directly proportional to the fuel consumed.

As seen in figure 5.19, the CO<sub>2</sub> emission does decrease as the CO<sub>2</sub> tax is increased. However, even with a CO<sub>2</sub> tax of 1000%, the emissions are only 92.6% of the emission with a -99% tax. This relatively low difference can be explained by the fact that the same amount of maintenance needs to be carried out. If a CTV decides to decrease the speed going out to a SM task that is not finished, it will have to finish at a later point, where additional fuel will be spent. Secondly, even for the -99% CO<sub>2</sub> case, the model will still conserve fuel by going slowly between points in some cases and still take the shortest optimal route. It can thus be argued that even in the -99% CO<sub>2</sub> tax case, the route is already optimized to reduce the distance travelled by the CTVs. Therefore, no matter the CO<sub>2</sub> tax applied the resultant emissions are already minimized, but are weighted relatively lower compared to revenue.

### Number of crew

As expected the number of crew in a maintenance setup determines how quickly the maintenance can be done. Figure 5.20 clearly shows how only 4, 5, and 6 crew combine with one CTV is able to perform enough maintenance to be done within the year, whereas fewer crews fail to finish within the year.

In the sensitivity analysis of the number of crews, the additional gain in performance using more than the minimum number of sufficient crew, does not justify the added salary costs of additional crews. One thing to note in this analysis is the use of a constant postponement penalty across runs. However as is seen in figure 5.20, the runs with a higher number of crews finishes much sooner than the others. As the postponement penalty defines the opportunity cost that the O&M model must be willing to sacrifice, the model regardless of the number of crews is equally willing to do maintenance. Thus if the

postponement costs are tuned such that each run finished at the same time the potential benefit of more crews would most likely be greater, and maybe worth it in regards to the added salary cost.

## Number of CTVs

While the number of crews determines how many maintenance task can be done at once, the number of CTVs determine how fast the crew can be placed at the maintenance tasks. For the case of an 18 turbines OWF there is a significant difference between having one or two CTVs. Adding a third CTV makes almost no difference, other than additional fuel usage and minimal gain to the revenue.

Given the results, once the minimum amount of CTVs needed to efficiently complete all maintenance is reached there is minimum added benefit of adding an additional CTV, again not justifying the extra associated costs of an additional CTV. This seems to follow the same logic as for the number of crews.

## 6.5 Effectiveness of optimization given PPAs or CFDs

Due to the use of power purchase agreements (PPAs) and contracts for difference (CFDs) in the sale of future power for a OWF operator, it is important to discuss whether opportunistically optimizing expected revenue is meaningful. In the case of Vattenfall, the owner of Kriegers Flak, as outlined in Vattenfalls Q1 Report 2024 (Vattenfall 2024), employ a hedge ratio of 55%. This effectively means, that before the power is produced they seek to have sold 55% at a predetermined price. This however means that the remaining 45% of the expected power remains unsold and will be sold in the day-ahead market. As the O&M activities impact a relatively small share of the total power production of the wind farm during a given hour, it can be argued that the saved revenue by the model comes from unhedged power production. This effectively means that for all cases where the power production is not fully hedged the PPAs or CFDs in place for a certain OWF should not have a significant impact on the effectiveness of the revenue-based opportunistic maintenance framework proposed in this study.

## 6.6 Broader impact

In general O&M cost account for around 25-30% of the cost of a wind farm (Röckmann, Lagerveld, and Stavenuiter 2017). Of the total O&M cost the lost revenue accounts for 38% according to Lochhead, Donnelly, and Carroll (2024). If this total lost revenue is reduced by around the 10% seen in figure 5.14D and 5.15D, it would results in a 1.14% reduction in life time cost of the wind farm, see equation 6.6.

$$\begin{aligned}
 \text{Reduction in costs} &= [\text{OWF lifetime cost}] \cdot [\text{O\&M share of lifetime cost}] \cdot \\
 &\quad [\text{Lost revenue share of O\&M cost}] \cdot [\text{Reduction in lost revenue}] \\
 &= [1] \cdot [0.3] \cdot [0.38] \cdot [(1 - 0.9)] = 1.14\%
 \end{aligned} \tag{6.1}$$

While this is an approximation, it does show the potential impact on the overall cost.

Reducing the O&M related costs of an OWF allows for a better investment opportunity for investors, as the associated value proposition will reflect a larger expected return of the wind farm. Thus a reduction in the lost revenue due to maintenance results in a lower levelized cost of electricity (LCOE).

Besides optimizing OWF O&M activities, the study has also shown that it is possible to generally place maintenance and production based on expectations for revenue for OWFs. The ability to strategically use power-market prices forecasts to optimize production might extrapolate to other renewable energy technologies such as Power-to-X (PtX) and solar power to maximize the revenue-based availability.

By improving the LCOE for offshore wind and showing that non-perfect price forecasts can help optimize production and potentially also for other renewable energy sources this study contributes to the expansion of renewable energy.

## 6.7 Key benefits of the proposed O&M model

Given the architecture of the proposed O&M model and the supporting results discussed, there are some elements that establish the novelty of the O&M model.

### Optimized revenue

As shown by the results the revenue-based O&M strategies outperform both naive and production-based O&M strategies. This is achieved by exploiting low revenue periods as opportunities to opportunistically place maintenance. This shows how there is an untapped potential within the offshore wind industry in adopting the novel revenue-based approach presented in this study.

### Reduced emissions

One of the key elements that differentiates this model compared to other models, is the modelling of the physical wind farm with the respective distances between turbines. This allows for a minimization of fuel costs when carrying out maintenance. In the simulations of the model, this is seen by CTVs sailing at a lower velocity and grouping of maintenance

tasks to reduce fuel usage. This allows an OWF operator to reduce emissions. Moreover an additional tuning of an emissions penalty can be incorporated to further reduce fuel usage with CO<sub>2</sub> emissions reduced by 8% in this study.

## Realistic O&M schedule

The quarterly-based maintenance schedule combined with the physical modelling of the OWF provides a realistic and detailed schedule for both CTVs and crews in regards to both CM and SM. This strengthens the trustworthiness of the O&M model when employed for simulating an O&M strategy.

## Consumption capacitated routing

Recently there has been a trend towards electrically driven CTVs (Conway 2024) in contrast to current combustion driven CTVs. This calls for several improvements and implementations into the current operations of OWF and the corresponding CTVs. As mentioned previously this model allows for a tracking of the consumption of a CTV. If a CTV has a limited electric capacity this could easily be taken into consideration as an additional constraint. This provides reassurance than an electrically driven CTV with limited range could be modelled and thereby incorporated into a revenue-based opportunistic maintenance strategy.

## 6.8 Model limitations

While the O&M model developed in this study provides a realistic simulation of maintenance operations due to its quarterly and physical model, it does have a range of limitations and assumptions that will have to be addressed when concluding on the results.

### Weather forecast

As described in section 4.3 the wind power forecast in this study is the actual weather with noise added in the form of a random walk. This would not be possible in a real-world setting. One thing to note with this approach is the fact that all optimization models run in this study used the same weather forecasts. Thus it can be argued that the relative difference in performance between models would still be realized, given actual weather forecasts.

This study assumed perfect knowledge of wave height which should be forecasted in a more realistic setup.

Furthermore, whenever a WSL is enforced it is solely based on the wind speed forecast. No mechanism is in place to deal with cases where no WSL is forecasted but the actual wind speed ends up reaching the WSL. There is also no mechanism to deal with cases when WSL is forecasted but the actual wind speed ends up being lower than the WSL.

Implementing this into the model would require spontaneity from the O&M operators. The level of this spontaneity would most likely be different for different OWF O&M teams making it difficult to model in a generalized way.

## Computational time

The computational time of the model with computational improvements including the matheuristic and arc lookout period, lies within a range that makes it possible to make daily schedule optimizations within a matter of seconds given a OWF size comparable to that of Kriegers Flak. When doing long term simulations the computational aspect becomes a significant challenge. If the O&M activities are to be simulated throughout a longer period such as 10 or 20 years with a sweep of the input parameters, the computational time would be on the order of days. If the model is to be used in this context, then several steps must be taken to achieve a further computationally optimized model.

A key limitation of this study is the fact that most results are only shown for up to 36 turbines whereas the full size of Kriegers Flak is 72 turbines. This was done to limit the computational time of the long-term simulations. Scaling the wind farm to 72 turbines not only requires approximately twice the amount of nodes, but also requires additional CTVs in order to perform the same amount of maintenance per turbine. Due to how the solve time scales with the number of turbines and CTVs as seen in section 5.3 and 5.6, this proved to be too computationally heavy to run for many simulations as required by the results section. While it is suspected that a size of 36 turbines is enough to generalize results, the revenue-based strategy performance on larger OWF sizes should be investigated before extrapolating results to full scale OWFs. In order to computationally allow for this using a reasonable amount of compute the suggestions in section 6.9 can be implemented. Note that the current implementation does allow for the optimization and scheduling of larger OWFs such as 72 turbines for single day cases, but requires on the order of 8 hours to do yearly simulations as seen in section 5.3.

## Crew simplification

As mentioned previously in section 4.4 one of the main assumptions in the model is that any crew can do any maintenance task, be it CM or SM of any type. In practice there would be different crews with different maintenance skills responsible for making repairs of different types.

## Maintenance simplification

In the model all SM is assumed to be the same and has no preferred order or minimum amount of maintenance for a single visit. In practice it is reasonable to assume that a minimum amount time should be allocated before maintenance is performed. Note that

in the proposed model, the implemented fuel cost prevents short windows of maintenance unless they are extraordinarily attractive. In practice once maintenance has started on a given turbine it should be prioritized before starting maintenance on other untouched turbines until all SM is performed on the initial turbine. However, due to the nature of the matheuristic implemented maintenance on turbines is performed in order of turbine number on days when no CM exists, as seen in figure 4.12A.

## OPEX realism

The proposed model does not directly include additional operational expenditures such as CTV leasing, crew salaries, etc. The expenditures can be included in the post processing of the results of a given simulation.

## Fixed O&M organisation

The amount of CTVs and crews are fixed parameters in the model and does not allow the model to make investments in additional crew or extra CTVs. Note that given the iterative simulation approach it is possible to split the simulation into periods with different input parameters allowing for different organisation sizes throughout the lifetime of the OWF.

## 6.9 Future work

Some of the limitations and assumptions outlined in section 6.8 could potentially be improved or amended, thus improving the realism of the O&M model. A major assumption of the model is the fact that any crew can do any form of maintenance task. This could be expanded in the current model, such that different crews exist with different purposes. This could potentially be based on the failures as defined in Carroll, McDonald, and McMillan (2016). Additionally, some of the failures should only be repairable by larger vessels such as JUVs or SOVs.

### HSE rule

Implementing the HSE rule stating that a CTV must be within 20 minutes of a deployed crew would further improve the realism of the O&M model. In the proposed model, this could be done by creating a constraint that ensures that at least one incoming arc into a predefined 20-minute distance zone surrounding the node where maintenance is being performed, is utilized in the next period, such that a CTV is always present in the 20-minute zone, when maintenance is being carried out.

### Real world validation

Another key element that would contribute to the reliability of the O&M model and its realism would be to validate the models results and compare the results to the O&M activities of a real world OWF. This should allow for further fine tuning of model pa-

rameters, which would provide a more reliable estimate for the potential savings from implementing the revenue-based O&M strategy outlined in this study.

### **Additional physical parameters**

Another factor that could contribute to the realism of the virtual model of the offshore wind farm, could be the inclusion of additional physical parameters. These parameters could include the offshore substations that would also need maintenance, the wake effects of the turbines, as well as potential prohibited zones with low water depth, marine life, etc..

### **Correlation between wind and power market prices**

As discussed in section 4.2, there is a negative correlation between the the wind speed and electricity prices in the DK2 electricity zone. Therefore low price periods are more likely to occur during high power periods. If there is little or no correlation between wind speeds and electricity prices, low price and low power periods would occur more often leading to a potential higher benefit of implementing the proposed revenue-based strategy. It would therefore be insightful to test the O&M model in an environment with low correlation between power market prices and wind power production, to investigate the effect of the correlation on the resultant performance.

### **Specialized loss function**

In the training of the models in this study, the RMSE is defined as the loss function. One could argue that another loss function could be defined that specializes the model to more accurately predict the hours of relative low prices as opposed to the absolute price level. This would come with several advantages such as the ability to define the hours of maintenance before running the optimization model. However it is also important to acknowledge the importance of having a reliable picture of the entire price development through the day.

### **Reduce solve time by full implementation of heuristic**

Currently the model is able to do long-term simulations in a reasonable amount of time for smaller OWF size but would struggle to do multi-year simulations for large OWFs with multiple CTVs. The matheuristic works by making the non-selected turbines inaccessible in the model using constraints. To additionally reduce the computation time, the model should only be defined for the selected turbines chosen by the matheuristic as described in algorithm 1. This will allow for a faster definition of the model, and a much faster solving time. Using this framework the solve time should not scale with the size of the OWF but rather only the number of turbines included in the matheuristic.

Exploring other ways of reducing the solve time would further help run simulations for

larger OWFs. This would allow for a more robust extrapolation of results to larger OWF sizes.

### **Solve clusters defined in heuristic independently**

As alluded to in section 6.2 future work could consist of creating clusters defined by the heuristic method for each CTV employed in the OWF. Given the nature of the heuristic, it could be beneficial to optimize the schedule for each of the clusters independently, which should allow the computational time to scale linearly with the number of CTVs.

## 6.10 Conclusion

The project aimed to quantify the potential benefit of opportunistically placing maintenance based on expectations for day-ahead power market prices and wind power production for O&M activities for an offshore wind farm. The O&M model is validated with a case study based on the location and layout of Kriegers Flak OWF connected to the DK2 Danish electricity zone. By building an O&M decision making framework based on an OR model using a time-space node approach this study is able to explore the differences in short-term decision making and long-term results for multiple O&M strategies. The developed O&M model is backtested using weather and power market data from the period of 2021 and 2022. To create power markets price forecasts a statistical model, ARIMAX, a machine learning model, ANN, and finally a exponentially weighted moving average, EWMA, of past prices were used. The forecasting methods were implemented in an OR model reflecting the physical layout of the OWF providing a detailed and realistic 15-minute based schedule for both CTV routing, crew placement, and maintenance activities.

The comparison between the different maintenance strategies highlighted that the short-term decision making can be improved by utilizing power market forecasts. The improved short-term decision making is also reflected in the long-term aggregated results, where an overall revenue increase is observed for the revenue-based strategies compared to a production-based strategy and naive methods not taking power production into account. The results from Kriegers Flak indicates a potential reduction in lost revenue due to SM of up to 79.4% compared to a naive scheduling method. The increased revenue for revenue-based strategies are obtained by accurately identifying frequently occurring low revenue periods throughout the year which are utilized to perform SM.

Additionally the modelling of the physical OWF as well as the routing of the CTVs resulted in an optimized schedule for a minimized level of GHG emissions based on a reduction in distances travelled by the CTVs as well as allowing slower transfer speeds.

In conclusion, the proposed O&M model offers a robust framework for optimizing O&M scheduling in offshore wind farms, enhancing operational efficiency, reducing costs, and supporting renewable energy growth.

# Bibliography

- Röckmann, Christine, Sander Lagerveld, and John Stavenuiter (Apr. 2017). “Operation and Maintenance Costs of Offshore Wind Farms and Potential Multi-use Platforms in the Dutch North Sea”. In:
- Erkan, Anil Çağlar, Enes Burak Ergüney, and Samet Gürsoy (2022). “The Energy Crises and Contagion from Europe to World: Evidence via Stochastic Volatility Model”. In: *International Journal of Business and Economic Studies*.
- Xia, Jiajun and Guang Zou (2023). “Operation and maintenance optimization of offshore wind farms based on digital twin: A review”. In: *Ocean Engineering*.
- Walger, Julia, Lennart Peters, and Reinhard Madlener (July 2017). *Economic Evaluation of Maintenance Strategies for Offshore Wind Turbines Based on Condition Monitoring Systems*. Tech. rep. FCN Working Paper.
- Wang, Jingjing, Xian Zhao, and Xiaoxin Guo (2019). “Optimizing wind turbine’s maintenance policies under performance-based contract”. In: *Renewable Energy*.
- Fallahi, F. et al. (2022). “A chance-constrained optimization framework for wind farms to manage fleet-level availability in condition based maintenance and operations”. In: *Renewable and Sustainable Energy Reviews*.
- Kang, Jichuan and C. Guedes Soares (2020). “An opportunistic maintenance policy for offshore wind farms”. In: *Ocean Engineering*.
- Papadopoulos, Petros, Farnaz Fallahi, et al. (2023). *Joint Optimization of Production and Maintenance in Offshore Wind Farms: Balancing the Short- and Long-Term Needs of Wind Energy Operation*.
- Lu, Yang et al. (2018). “Condition based maintenance optimization for offshore wind turbine considering opportunities based on neural network approach”. In: *Applied Ocean Research*.
- Erguido, A. et al. (2017). “A dynamic opportunistic maintenance model to maximize energy-based availability while reducing the life cycle cost of wind farms”. In: *Renewable Energy*.
- Besnard, François, Katharina Fischer, and Lina Bertling Tjernberg (Apr. 2013). “A Model for the Optimization of the Maintenance Support Organization for Offshore Wind Farms”. In: *Sustainable Energy, IEEE Transactions on*.
- McMorland, J. et al. (2023). “Opportunistic maintenance for offshore wind: A review and proposal of future framework”. In: *Renewable and Sustainable Energy Reviews*.
- Li, Mingxin et al. (2020). “An opportunistic maintenance strategy for offshore wind turbine system considering optimal maintenance intervals of subsystems”. In: *Ocean Engineering*.

- Papadopoulos, Petros, David W. Coit, and Ahmed Aziz Ezzat (2022). *STOCHOS: Stochastic Opportunistic Maintenance Scheduling For Offshore Wind Farms*.
- Lago, Jesus et al. (2021). "Forecasting day-ahead electricity prices: A review of state-of-the-art algorithms, best practices and an open-access benchmark". In: *Applied Energy*.
- Carrol, James, Alasdair McDonald, and David McMillan (2016). *Failure rate, repair time and unscheduled O&M cost analysis of offshore wind turbines - Carroll - 2016 - Wind Energy - Wiley Online Library*. <https://onlinelibrary.wiley.com/doi/full/10.1002/we.1887>.
- Kallehauge, Brian et al. (2005). "Vehicle Routing Problem with Time Windows". In: *Column Generation*. Ed. by Guy Desaulniers, Jacques Desrosiers, and Marius M. Solomon. Boston, MA: Springer US.
- Zhang, Dong et al. (2017). "A time-space network flow approach to dynamic repositioning in bicycle sharing systems". In: *Transportation Research Part B: Methodological*.
- Irawan, Chandra Ade et al. (2017). "Optimisation of maintenance routing and scheduling for offshore wind farms". In: *European Journal of Operational Research*.
- Pisinger, David and Stefan Røpke (2007). "A general heuristic for vehicle routing problems". In: *Computers & Operations Research*.
- Wang, Keke et al. (2023). "Short-term electricity price forecasting based on similarity day screening, two-layer decomposition technique and Bi-LSTM neural network". In: *Applied Soft Computing*.
- Ziel, Florian and Rick Steinert (2018). "Probabilistic mid- and long-term electricity price forecasting". In: *Renewable and Sustainable Energy Reviews*.
- Esteves, Gheisa et al. (Dec. 2015). "Long Term Electricity Forecast: A Systematic Review". In: *Procedia Computer Science*.
- Pessanha, José Francisco Moreira and Nelson Leon (2015). "Forecasting Long-term Electricity Demand in the Residential Sector". In: *Procedia Computer Science*.
- Conejo, Antonio J. et al. (2005). "Forecasting electricity prices for a day-ahead pool-based electric energy market". In: *International Journal of Forecasting*.
- Tsai, Wen-Chang et al. (2023). "A Review of Modern Wind Power Generation Forecasting Technologies". In: *Sustainability*.
- European Centre for Medium-Range Weather Forecasts (2024). *Medium-Range Forecasts Documentation and Support*. <https://www.ecmwf.int/en/forecasts/documentation-and-support/medium-range-forecasts>.
- Lam, Remi et al. (2023). *GraphCast: Learning skillful medium-range global weather forecasting*.
- Pathak, Jaideep et al. (2022). *FourCastNet: A Global Data-driven High-resolution Weather Model using Adaptive Fourier Neural Operators*.
- Bi, Kaifeng et al. (2022). *Pangu-Weather: A 3D High-Resolution Model for Fast and Accurate Global Weather Forecast*.

- Diaconita, Alexandra, Gabriel Andrei, and Liliana Rusu (Dec. 2022). “An overview of the offshore wind energy potential for twelve significant geographical locations across the globe”. In: *Energy Reports*.
- Hersbach, H. et al. (2023). *ERA5 hourly data on single levels from 1940 to present*.
- ENTSO-E (2024). *ENTSO-E Transparency Platform API*. <https://transparency.entsoe.eu/>.
- Schermeyer, Hans, Claudio Vergara, and Wolf Fichtner (2018). “Renewable energy curtailment: A case study on today’s and tomorrow’s congestion management”. In: *Energy Policy*.
- Nycander, Elis et al. (2020). “Curtailment analysis for the Nordic power system considering transmission capacity, inertia limits and generation flexibility”. In: *Renewable Energy*.
- Ben-Bouallegue, Zied et al. (Apr. 2022). *Statistical modelling of 2m temperature and 10m wind speed forecast errors*. eng.
- Lindemann, Benjamin et al. (2021). “A survey on long short-term memory networks for time series prediction”. In: *Procedia CIRP*.
- Chen, Tianqi and Carlos Guestrin (Aug. 2016). “XGBoost: A Scalable Tree Boosting System”. In: *Proceedings of the 22nd ACM SIGKDD International Conference on Knowledge Discovery and Data Mining*. KDD ’16. ACM.
- Cavanaugh, Joseph and Andrew Neath (Mar. 2019). “The Akaike information criterion: Background, derivation, properties, application, interpretation, and refinements”. In: *Wiley Interdisciplinary Reviews: Computational Statistics*.
- Xiong, Xiaoping and Guohua Qing (2023). “A hybrid day-ahead electricity price forecasting framework based on time series”. In: *Energy*.
- Gusti, A. P. and Semin (2016). “The Effect of Vessel Speed on Fuel Consumption and Exhaust Gas Emissions”. In: *American Journal of Engineering and Applied Sciences*.
- Jordan, Jack and Martyn Lasek (n.d.). *FEATURE: 10 Years of Bunker Prices - Ship & Bunker*. <https://shipandbunker.com/news/world/366958-feature-10-years-of-bunker-prices>.
- Windcat 42 / FRS Windcat Offshore Logistics* (n.d.). <https://www.fwol.de/en/fleet/windcat-42>.
- Meyer, Jasper, Robert Stahlbock, and Stefan Voss (Jan. 2012). “Slow Steaming in Container Shipping”. In: *International Conference on System Sciences*.
- Technical University of Denmark (2024). *High Performance Computing*. [https://www.hpc.dtu.dk/?page\\_id=2520](https://www.hpc.dtu.dk/?page_id=2520).
- Cortesi, Nicola et al. (2019). “Characterization of European wind speed variability using weather regimes”. In: *Climate Dynamics*.

*Marine Benchmark: 2020 global shipping CO<sub>2</sub> emissions down 1% - Offshore Energy* (n.d.). <https://www.offshore-energy.biz/marine-benchmark-2020-global-shipping-co2-emissions-down-1/>.

Schäschke, Carl, Isobel Fletcher, and Norman Glen (2013). “Density and Viscosity Measurement of Diesel Fuels at Combined High Pressure and Elevated Temperature”. In: *Processes*.

Anstreicher, K. et al. (2024). *Decision Tree for Optimization Software*. <https://plato.asu.edu/bench.html>.

TV2 (2022). *Her er strømmen næsten gratis lørdag*. (Visited on 07/05/2024).

Vattenfall (2024). *q1\_report\_2024.pdf*. [https://group.vattenfall.com/siteassets/corporate/investors/interim\\_reports/2024/q1\\_report\\_2024.pdf](https://group.vattenfall.com/siteassets/corporate/investors/interim_reports/2024/q1_report_2024.pdf).

Lochhead, Robert, Orla Donnelly, and James Carroll (2024). “System-Level Offshore Wind Energy and Hydrogen Generation Availability and Operations and Maintenance Costs”. In: *Wind*.

Conway, Martin (May 2024). *End of an era for diesel-powered CTVs*. <https://rina.org.uk/publications/ship-and-boat-international/end-of-an-era-for-diesel-powered-ctvs/>.

# A Appendix

## A.1 Detailed tables

Table A.1: Architecture of the LSTM Model

Layer	Parameters	Description
Input	Shape: (Training length, features)	Input layer
Bi-LSTM	Units: 128, Return Seq: True	First bidirectional LSTM block
Dropout	Rate: 0.1	Prevent over fitting
Bi-LSTM	Units: 128, Return Seq: True	Second LSTM block with residual connection
Dropout	Rate: 0.1	Prevent overfitting
Add	-	Adds residual connection
Bi-LSTM	Units: 128, Return Seq: True	Third bidirectional LSTM block
Dropout	Rate: 0.1	Prevent over fitting
Bi-LSTM	Units: 128, Return Seq: False	Fourth LSTM block
Dropout	Rate: 0.1	Prevent over fitting
Dense	Units: 256, Act: ReLU	Dense layer
Dropout	Rate: 0.1	Prevent over fitting
Dense	Units: 128, Act: ReLU	Second dense layer
Dropout	Rate: 0.1	Prevent over fitting
Dense	Units: 24	Output layer
Reshape	Shape: (24, 1)	Reshape to 24-hour forecast

Table A.2: Orders used to train ARIMAX model and the corresponding AIC values

<b>Order</b> $(p, d, q)$	<b>AIC</b>						
(0, 0, 0)	45578.7707	(0, 0, 1)	20828.2935	(0, 0, 2)	7996.1884	(0, 0, 3)	1627.2580
(0, 0, 4)	-1663.9425	(0, 0, 5)	-3861.2792	(0, 1, 0)	-8046.4243	(0, 1, 1)	-8622.1899
(0, 1, 2)	-8662.2388	(0, 1, 3)	-8849.7994	(0, 1, 4)	-8950.4220	(0, 1, 5)	-9033.8575
(1, 0, 0)	-8360.8404	(1, 0, 1)	-9091.2422	(1, 0, 2)	-9093.2751	(1, 0, 3)	-9184.9389
(1, 0, 4)	-9231.2603	(1, 0, 5)	-9273.2446	(1, 1, 0)	-8550.9439	(1, 1, 1)	-8637.7774
(1, 1, 2)	-9353.4812	(1, 1, 3)	-9374.0911	(1, 1, 4)	-9375.7502	(1, 1, 5)	-9370.1345
(2, 0, 0)	-9031.0306	(2, 0, 1)	-9089.2650	(2, 0, 2)	-9424.3550	(2, 0, 3)	-9179.3264
(2, 0, 4)	-9445.2091	(2, 0, 5)	-9438.4207	(2, 1, 0)	-8725.6025	(2, 1, 1)	-9366.7527
(2, 1, 2)	-9370.5230	(2, 1, 3)	-9374.6642	(2, 1, 4)	-9373.9551	(2, 1, 5)	-9372.7044
(3, 0, 0)	-9129.4867	(3, 0, 1)	-9082.6754	(3, 0, 2)	-9442.8036	(3, 0, 3)	-9157.0673
(3, 0, 4)	-9454.3568	(3, 0, 5)	-9450.1307	(3, 1, 0)	-8841.4968	(3, 1, 1)	-8830.4529
(3, 1, 2)	-9362.9957	(3, 1, 3)	-9369.9938	(3, 1, 4)	-9367.7992	(3, 1, 5)	-9379.7191
(4, 0, 0)	-9191.7073	(4, 0, 1)	-9172.1563	(4, 0, 2)	-9162.4669	(4, 0, 3)	-9154.7189
(4, 0, 4)	-9435.2294	(4, 0, 5)	-9346.7449	(4, 1, 0)	-8884.9255	(4, 1, 1)	-8874.9343
(4, 1, 2)	-9376.3749	(4, 1, 3)	-9374.8990	(4, 1, 4)	-9363.9745	(4, 1, 5)	-9376.2048
(5, 0, 0)	-9209.5183	(5, 0, 1)	-9194.4798	(5, 0, 2)	-9181.4391	(5, 0, 3)	-9495.6582
(5, 0, 4)	-9306.5932	(5, 0, 5)	-9470.3855	(5, 1, 0)	-8977.6199	(5, 1, 1)	-8964.1185
(5, 1, 2)	-9373.0013	(5, 1, 3)	-9371.1980	(5, 1, 4)	-9625.5981	(5, 1, 5)	-9394.9381

Table A.3: Run parameters for solve and memory load test.

Parameter	Value
Days	15
W	6-72
Day start	1
Price quantile	80th
SM per turbines [quarters]	160
Turbines in heuristic. See sec. 4.4	6
Forecast	EWMA
CTVs	1
Crews	4
Year	2021
<b>Compute parameters</b>	
Compute resource	Lenovo ThinkSystem SD530
RAM	32GB
Cores	16

Table A.4: Optimization solver performance data comparison between Gurobi and Highs

Nr. of turbines	Gurobi Solve Time	Gurobi Model Defi-nition Time	Gurobi Max Mem	Highs Solve Time	Highs Model Defi-nition Time	Highs Max Mem
6	23	35	108	464	53	1392
12	30	43	326	95	127	1604
18	44	43	735	109	372	1902
24	103	70	2705	964	901	2869
30	107	67	3429	1130	1498	3912
36	178	110	4698	-	-	-
54	361	199	14228	-	-	-
72	785	320	25722	-	-	-

## A.2 Unit check

**Objective Function:**

$$\max \left\{ \sum_{\forall t \in T} \sum_{\forall w \in W} x_{t,w} [\text{dimensionless}] \cdot \Theta_w(w s_t) [\text{MWh}] \cdot p_t [\text{€/MWh}] - MC_t [\text{€}] - PP [\text{€}] \right\} \quad (\text{A.1})$$

**Realized profit:**

$$\Pi [\text{€}] = \sum_{\forall t \in T} \sum_{\forall w \in W} x_{t,w} [\text{dimensionless}] \cdot \Theta_w(W S_t) [\text{MWh}] \cdot \pi_t [\text{€/MWh}] - MC_t [\text{€}] \quad (\text{A.2})$$

**Constraints:** Note that only constraints containing units are included.

$$MC_t [\text{€}] = FC [\text{€/L}] \sum_{s,t,r,t'} C_{s,r,\Delta t} [\text{L}] \cdot A_{s,t,r,t'} [\text{dimensionless}] \quad (\text{A.3})$$

$$h_{t,w}^{CM} [\text{Quarters}] \leq (1 - x_{t,w} [\text{dimensionless}]) \cdot M_{cm} [\text{Quarters}] \quad (\text{A.4})$$

$$h_{1,w}^{CM} [\text{Quarters}] = H_w^{CM} [\text{Quarters}] - r_{1,w}^{CM} [\text{Quarters}] \quad (\text{A.5})$$

$$h_{1,w}^{SM} [\text{Quarters}] = H_w^{SM} [\text{Quarters}] - r_{1,w}^{SM} [\text{Quarters}] \quad (\text{A.6})$$

$$h_{t+1,w}^{CM} [\text{Quarters}] = h_{t,w}^{CM} [\text{Quarters}] - r_{t,w}^{CM} [\text{Quarters}] \quad (\text{A.7})$$

$$h_{t+1,w}^{SM} [\text{Quarters}] = h_{t,w}^{SM} [\text{Quarters}] - r_{t,w}^{SM} [\text{Quarters}] \quad (\text{A.8})$$

$$wh_t [\text{m}] \leq WHL [\text{m}] + M_{limit} [\text{m}] \cdot Z_{ctv,t,|W|+ctv} \quad (\text{A.9})$$

$$wh_t [\text{m}] \leq WHL [\text{m}] + M_{wh\_limit} [\text{m}] \cdot (1 - \sum_{w \in W} r_{t,w}^{SM} + r_{t,w}^{SM}) \quad (\text{A.10})$$

$$ws_t [\text{m/s}] \leq WSL [\text{m/s}] + M_{limit} [\text{m/s}] \cdot Z_{ctv,t,|W|+ctv} \quad (\text{A.11})$$

$$ws_t [\text{m/s}] \leq WSL [\text{m/s}] + M_{ws\_limit} [\text{m/s}] \cdot (1 - \sum_{w \in W} r_{t,w}^{SM} + r_{t,w}^{SM}) \quad (\text{A.12})$$

$$PP [\text{€}] = \sum_{\forall w \in W} h_{|T|,w}^{SM} [\text{Quarters}] \cdot \frac{PP_{cost}^{SM} [\text{€/Hour}]}{4 [\text{Quarters/Hour}]} + h_{|T|,w}^{CM} [\text{Quarters}] \cdot \frac{PP_{cost}^{CM} [\text{€/Hour}]}{4 [\text{Quarters/Hour}]} \quad (\text{A.13})$$

$$A_{s,t,r,t'} [\text{dimensionless}] \leq \max(0, (t' [\text{Quarters}] - t [\text{Quarters}]) - D_{s,r} [\text{Quarters}]) \quad (\text{A.14})$$

## A.3 GitHub Link

[https://github.com/JohanKnarreborg/OWF\\_OM\\_OPTIMIZATION](https://github.com/JohanKnarreborg/OWF_OM_OPTIMIZATION)